Agriculture, Ecosystems and Environment 380 (2025) 109388

Contents lists available at ScienceDirect

Agriculture, Ecosystems and Environment

journal homepage: www.elsevier.com/locate/agee

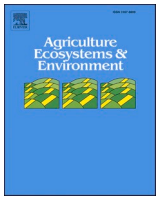

# Soil organic matter quality in an olive orchard differently managed for 21 years: Insights into its distribution through soil aggregates and depth

Rosangela Addesso [a], Fabrizio Araniti [b], Andrea Bloise [c], Alba N. Mininni [a], Bartolomeo Dichio [a], David López-González [d,e], Hazem S. Elshafie [a], Ruth H. Ellerbrock [f], Laura S. Schnee [g], Juliane Filser [h], Domenico Sileo [a], Adriano Sofo [a,*]

[a] Department of Agricultural, Forestry, Food and Environmental Sciences (DAFE), University of Basilicata, Viale dell'Ateneo Lucano 10, Potenza 85100, Italy
[b] Department of Agricultural and Environmental Sciences - Production, Landscape, Agroenergy, University "Statale" of Milan, Via Celoria 2, Milan 20133, Italy
[c] Department of Biology, Ecology and Earth Sciences, University of Calabria, Via Pietro Bucci, Rende, CS 87036, Italy
[d] Instituto de Agroecoloxía e Alimentación (IAA), Universidade de Vigo, Campus Auga, Ourense 32004, Spain
[e] Departamento de Bioloxía Vexetal e Ciencia do Solo, Facultade de Bioloxía. Universidade de Vigo, Campus Lagoas-Marcosende s/n, Vigo 36310, Spain
[f] Leibniz Centre for Agricultural Landscape Research (ZALF), Eberswalder Straße 84, Müncheberg 15374, Germany
[g] Institute for Mineralogy, Leibniz University of Hannover, Callinstraße 3-9, Hannover 30167, Germany
[h] Center for Environmental Research and Sustainable Technology (UFT), University of Bremen, Leobener Str 6, Bremen 28359, Germany

ARTICLE INFO

*Keywords:*
Aggregate-associated organic matter
Soil metabolomics
Soil mineralogy
Sustainable soil management
Fourier-transform infrared (FTIR) spectroscopy

ABSTRACT

Among the current global challenges, the research of new practices aimed at mitigating soil impoverishment, exacerbated by the pressing climate changes, is the most urgent. Studying soil organic matter (SOM) ecological dynamics and comparing the conventional intensive farming practices with the emerging alternative sustainable ones can represent a key indicator in soil health investigation, helping to find new guidelines for conservative agrosystems management. In this study, the soil from a Mediterranean olive orchard, with both sustainable ($S_{mng}$) and conventional ($C_{mng}$) land use for 21 years, was investigated for its physicochemical properties, with a particular attention to the soil organic matter from aggregates (SOM-A) and its interaction and distribution at different soil depths. Significantly higher amounts of total carbon (+50.7 %) and nitrogen (+74.9 %), as well as of SOM-A aromatic component (+76.0 %), were detected in the topsoil layer (0–5 cm) of the $S_{mng}$, compared to the $C_{mng}$, a sign that the organic matter from surface deeply seeps slowly. This evidence was highlighted especially in micro-aggregates (< 0.063 mm) of the $S_{mng}$, compared to the $C_{mng}$ (C = +59.3 %; N = +86.7 %; SOM-A aromatic component = +87.7 % in the $S_{mng}$). This trend was also reflected in an increase in the bacterial abundance and in a different accumulation of organic compounds deriving from microbial fermentation processes in $S_{mng}$ soil, as highlighted by the SOM-A qualitative characterization by metabolomics. The soil mineralogical analysis showed that minerals maintained a higher crystallinity in the $S_{mng}$ than in the $C_{mng}$, where soil tillage promoted their alteration. Moreover, Fourier-transform infrared (FTIR) spectroscopy analysis highlighted that soil disturbance in the $C_{mng}$ can affect SOM distribution, creating different spatial distributions in the particle aggregates and soil depths. Distinguishing SOM quantity, quality, and interaction with mineral components can help to understand its degradability and dynamics, both essential for mitigating the effects of climate change and promoting land protection.

## 1. Introduction

Currently, climate change, the lack of resources and the increase of world population, with the consequent growing demand for food, entails the urgent need of sustainable, regenerative and conservative agricultural practices able to combat soil pauperization and degradation (Chittora et al., 2020; Kalyanasundaram et al., 2020; Gonçalves, 2021; Tan et al., 2021). Soil organic matter (SOM) can be of pivotal importance to understand the soil ecological dynamics because underpins soil health (Doran and Parkin, 1994; Doran and Zeiss, 2000). This latter is like a three-legged stool: physical, chemical, and biological components sustain soil health, with each one affecting the others. The

* Corresponding author.
*E-mail address:* adriano.sofo@unibas.it (A. Sofo).

https://doi.org/10.1016/j.agee.2024.109388
Received 17 February 2024; Received in revised form 16 November 2024; Accepted 17 November 2024
Available online 22 November 2024

corresponding indicators, including soil texture, bulk density, pH, organic carbon quantity and quality, microbial diversity and activities, can have a crucial role in the soil health assessment (Fierer et al., 2021).

Specifically, SOM is considered the most important terrestrial carbon stock and source of soil nutrients, whose increase is associated with higher agricultural yields, with a crucial role in food security issues (Canisares et al., 2023; Li et al., 2023; Kane et al., 2021). The SOM is mainly formed (1) via fragmentation of the above-ground plant and animal residues; (2) by exudates from plant roots; (3) by mineral and organic fertilization; (4) by other carbon inputs (such as pruning residues, fallen/thinned olives and leaves, cover crop residues, and residues from olive oil production); (5) by the living soil biomass (especially microbial). These sources of SOM can regulate soil nutrient availability, aggregate stability, carbon sequestration and pollutant degradation, and plant disease prevalence and plant growth promotion (González-Pérez et al., 2005; Prescott and Vesterdal, 2021; Whalen et al., 2022). The crop type, as well as the soil tillage and management, influences SOM formation processes and SOM stability, modulating qualitatively and quantitatively its supplies and the relative decomposition rates. In particular, grassing and organic land use under long-term cause increases in SOM amount (Pulleman et al., 2000; Leifeld and Kögel-Knabner, 2005; Haghighi; Guimarães et al., 2013). Consequently, this capacity of the soil to preserve and store organic carbon depends on many factors, such as soil type, soil mineralogy, soil depth, and climate (Yeasmin et al., 2023).

In Mediterranean climates, often influenced by water scarcity and high temperatures - factors today exacerbated by the pressing climate change - soil health in orchard agroecosystems is endangered by erosion and loss of fertility (Iglesias et al., 2007; Keesstra et al., 2016; Sofo and Palese, 2021). Olive is an economically and socio-culturally important tree crop for the countries of the Mediterranean area, being part of the Mediterranean triad, together with vine and wheat. However, its management is becoming unsustainable because of the lack of young farmers, increasing soil degradation, and the high cost of mineral fertilizers. Among the sustainable practices that can be adopted to reverse this negative trend, no- or minimum tillage, localized irrigation, and managing carbon inputs internal to the orchard have a special role (Sofo and Palese, 2021). At the olive orchard level, a healthy soil rich in organic matter can be a crucial driver for olive productivity and profitability in the long term, providing a wide range of ecosystem services (González-Pérez et al., 2005; Benitez et al., 2006).

This research aims at characterizing the soil chemical, physical and microbiological features, with a particular attention to the composition of soil organic matter from aggregates (SOM-A) and to its interactions with soil mineral components in a Mediterranean olive orchard differentially managed (sustainably and conventionally) for 21 years. More specifically, we examined (i) the essential elements content (carbon and nitrogen), (ii) mineralogical soil composition, (iii) SOM-A quanti-qualitative analysis, including the study of metabolites, and (v) bacterial abundance in the topsoil (0–30 cm) considering three different depths (0–5, 5–15, 15–30 cm) and three aggregate size classes (1–0.250, 0.250–0.063, $<$ 0.063 mm) with the scope to highlight their management-driven variability. We hypothesized that SOM dynamics could have been influenced by the two different agricultural practices applied for a long term in the field.

## 2. Materials and methods

### 2.1. Geological setting, experimental field and its management

The site under study is in a basin of foredeep deposits of the Pliocene-Pleistocene age (i.e., Bradanic depression), which lies partly on the southern Apennine front. The Bradanic Depression deposits consist primarily of sea sands and conglomerates. In the investigated area, the Basento watercourse, with its SE-oriented beds, cuts through the marine terraces and the underlying layers of silt and clay from the Pleistocene (Bentivenga et al., 2004). The land under study falls within the municipality of Ferrandina and is on the fluvial terraces of the Basento valley, formed by Holocene alluvial sands with a predominantly siliceous composition and conglomerates (Supplementary Fig. S1).

The trial was conducted in a 2-ha mature olive grove (*Olea europaea* L., cv. 'Maiatica'; plants with an age of approximately 70 years, trained to vase at a distance of 8 $\times$8 m; NE orientation) in Ferrandina (Southern Italy, Basilicata region; N 40°29', E 16°28') and split into two plots, one managed using sustainable (sustainable management, $S_{mng}$) and the other with conventional agricultural practices (conventional management, $C_{mng}$) (Supplementary Figs. S2 and S3). The area is characterized by a warm temperate, dry climate, with an annual rainfall of 540 mm (mean 1995–2019) and a mean annual temperature of 16.2 °C. The soil is a sandy loam, Haplic Calcisol, with sediment as parental material (Lal, 2017; Sofo and Palese, 2021).

Sustainable techniques have been adopted for 21 years (starting in 2000) in a mature olive orchard to conserve and improve soil organic matter content, maintaining olive tree productivity. The $S_{mng}$ area was drip-irrigated (on average, 2850 $m^3$ $ha^{-1}$ $yr^{-1}$) from March to October, with urban wastewater treated by a pilot unit (Palese et al., 2009; Sofo et al., 2019). The average values (mean 2000–2019) of organic N, P and K distributed through the treated wastewater were 52, 4 and 49 kg $ha^{-1}$ $yr^{-1}$, respectively, and an integrative amount of 40 kg $ha^{-1}$ $yr^{-1}$ of $N\text{-}NO_3^-$ was distributed in the early spring to satisfy plant nutrient needs (Sofo and Palese, 2021). The soil was no-tilled. The soil was permanently covered by spontaneously self-seeding weeds mowed at least twice a year. A light pruning was performed yearly during winter to reach the vegetative-reproductive balance of the trees. Pruning and grassing residuals were shredded and left along the row as mulch.

The adjacent $C_{mng}$ plot (1 ha) was kept as a control and treated conventionally: it was rain-fed, fertilized once per year in the early spring with mineral N, P and K in amounts of 80, 10 and 40 kg $ha^{-1}$ $yr^{-1}$, respectively. Soil was managed by tillage (harrowing up to 10 cm soil depth) performed 2–3 times per year to control weeds. Intensive canopy pruning was performed every two years. Pruning and grassing residuals were removed from the olive orchard (Sofo and Palese, 2021). Table 1 summarizes the two land use systems.

The main physicochemical properties of the topsoil layers (0–5, 5–15, and 15–30 cm depth) in the $S_{mng}$ and $C_{mng}$ systems are reported in Supplementary Table S1. There were no diseases, biotic stresses, nor N and P deficiency symptoms in the trees of both the management systems. There were no significant differences in tree height (about 4.0–4.5 m) and trunk diameter between $S_{mng}$ and $C_{mng}$ trees. In the $S_{mng}$ system, higher olive yield occurred compared to the $C_{mng}$ system (8.2 *vs* 6.0 t

**Table 1**
Comparison between the sustainable ($S_{mng}$) and conventional ($C_{mng}$) practices applied in the olive orchard.

| Practice | Sustainable ($S_{mng}$) | Conventional ($C_{mng}$) |
|---|---|---|
| ***Irrigation Fertilization*** | Ferti-drip irrigation (2850 $m^3$ $ha^{-1}$ $yr^{-1}$) with treated urban wastewater (NPK: 50, 4 and 49 kg $ha^{-1}$ $year^{-1}$), from March to October + mineral $N\text{-}NO_3$ (40 kg $ha^{-1}$ $yr^{-1}$), in the early spring | Rain-fed<br>Mineral fertilization (80, 10 and 40 kg $ha^{-1}$ $year^{-1}$), once per year in the early spring |
| ***Soil tillage*** | No tillage | Harrowing (10 cm depth), 2–3 times per year |
| ***Grassing*** | Spontaneously self-seeding weeds | No grassing |
| ***Grassing residuals management*** | Mowed twice a year, left on the field as mulch | - |
| ***Pruning*** | Light pruning, yearly during winter | Intensive canopy pruning, every two years |
| ***Pruning residuals management*** | Shredded and left on the fields as mulch | Removed from the orchard and burned |

ha$^{-1}$ yr$^{-1}$, mean 2001–2019) (Sofo and Palese, 2021).

### 2.2. Soil sampling, aggregate size distribution and C/N measurements

In August 2021, soil sampling was performed in the row area of both systems ($S_{mng}$ and $C_{mng}$) at about 130 cm from the trunk in the soil wetted by fertigation of the $S_{mng}$ and in the corresponding positions in the $C_{mng}$. Three trenches (40 × 50 cm) in three different parts of the fields were excavated with a hoe and, for each trench, 10 soil sub-samples were picked at three different soil depths (0–5, 5–15 and 15–30 cm) (Supplementary Fig. S4). The 10 sub-samples were taken in proximity and pooled on site to make up a composite soil sample of about 1.0 kg. Therefore, for each soil management systems ($S_{mng}$ and $C_{mng}$), three composite samples for each soil depth (0–5, 5–15 and 15–30 cm) (18 composite samples in total) were collected and carefully transported at the laboratory to avoid the disruption of the aggregates. This sampling technique allowed for minimal spatial variability, according to Sofo et al. (2019). After removing visible crop residues, the soil composite samples were immediately stored in sterilized plastic bags and stored at 4 °C for chemical analyses. After three days, soil samples were transferred from plastic bags to plastic trays and let dry in a cold room (5 °C) for 14 days before sieving.

The dry sieving was conducted with a sequential iron sieve series (5, 2, 1, 0.250 and 0.063 mm) (Flinn Scientific Inc., Hamilton, ON, Canada) shaken manually for 3 min. This allowed to separate six aggregate size classes (>5, 5–2, 2–1, 1–0.250, 0.250–0.063, and < 0.063 mm) that were placed plastic containers. An aliquot (5 g) of each aggregate sample was inserted in ceramic crucibles, weighted, desiccated for 24 h at 105 °C, placed in a desiccator containing silica gel until a constant weight was reached, and then weighted again to calculate the percentage of water loss. Based on this latter value, the aggregate samples were entirely weighted and the resulting weight was corrected by removing the percentage of water. The aggregate class distribution in the two treatments at each of the three soil depths was calculated.

The smaller aggregate size classes (1–0.250, 0.250–0.063, and 0.063 mm) were analyzed, with 54 samples (2 soil management types × 3 soil depths × 3 aggregate size classes × 3 composite sample replicates). Successively, each soil sample was ground for 5 min using a mixer (model ProMix 800 W; Koninklijke Philips N.V., Amsterdam, The Netherlands), and the resulting powder was used for the analysis of soil total carbon (STC) and soil total nitrogen (STN). Aluminum capsules containing approximately 20–30 mg of the ground soil were used for STC and STN elemental determination by a C-N analyzer (model CN 802; Velp Scientifica, Usmate Velate MB, Italy) and the results were expressed on a weight basis. The remaining soil not used for STC and STN measurements was powdered (particle size of approximately 10 μm) using a bead beater Mixer Mill MM 200 made of stainless steel (Retsch Technology, Düsseldorf, Germany) at 18 Hz for 1 min and then at 25 Hz for 1 min, and used for the following analysis.

### 2.3. X-ray powder diffraction (XRPD) mineralogical analysis

To characterize the mineralogical properties of the finely ground soil samples was performed on all samples by X-ray Powder Diffraction (XRPD), through a Bruker D8 Advance diffractometer (Bruxer Co., Billerica, MA, USA), with Cu-Ka radiation, operating at 40 kV and 40 mA. Scans were collected between 3°-66° 2θ using a step interval of 0.02° 2θ with a step counting time of 0.2 s. The EVA software program (DIFFRACplus EVA; Bruker Co.) identified the mineralogical phases in each X-ray powder spectrum by comparing experimental peaks with PDF2 reference patterns. An assessment of the semi-quantitative mineralogical abundance present in the samples were attained by Rietveld refinements (Gualtieri et al., 2019; Addesso et al., 2022), using TOPAS software V.4.2 (Bruker Co.). Crystallinity of minerals was evaluated by the evolution of the full width at half-maximum (FWHM) of the main reflection (hkl) on XRPD patterns.

### 2.4. Fourier-transform infrared (FTIR) spectroscopy analysis

To evaluate the SOM variabilities in its composition, the finely ground soil samples were analyzed with Fourier-transform infrared (FTIR) spectroscopy using the KBr technique (Ellerbrock and Gerke, 2013). Briefly, 1 mg of the sample was mixed with 99 mg of potassium bromide (KBr), stored overnight in an exsiccator, finely ground using an agate mortar, and pressed into pellets (Ellerbrock et al., 1999). The pellets were analyzed using an FTS135 spectrometer (BioRad Corp, Hercules, CA, USA). All spectra were recorded in absorption mode at a resolution of 2 cm$^{-1}$ by using 16 scans (i.e., 16 co-added single spectra), corrected against ambient air as background (Haberhauer and Gerzabek, 1999), and smoothed using a "boxcar"-function (factor 25; Bio-Rad Winirez software; Bio-Rad Laboratories Inc., Hercules, CA, USA). The baseline-corrected spectra were interpreted as Ellerbrock et al. (1999) described using Biorad Winirez software. The absorption maximum of the C-O-C band was found in the WN range of 1100–1000 cm$^{-1}$, in accordance with the range reported by Ellerbrock et al. (1999) for arable soil samples. The region of the maximum of the $COO^-$ band ($WN_{COO^-}$) was found from WN 1690–1560 cm$^{-1}$ (Celi et al., 1997), and the one of the $OM_{cat}$ band was found in the region from WN 1440–1400 cm$^{-1}$ (Alvarez-Puebla et al., 2005).

### 2.5. Organic matter from aggregates (SOM-A) quantification and metabolomic analysis

For SOM-A desorption, stabilized within aggregates, the finely ground soil samples (350 mg for each sample) were placed in Eppendorf tubes, and 1 mL of 0.01 M NaCl brought to pH 4 with HCl was added (Mikutta et al., 2007). The tubes were placed in a horizontal shaker for 20 h at 90 rpm and then centrifuged for 30 min at 12,000 ×*g*. The supernatant was taken and immediately read at 280 nm (absorption peak for aromatic rings) by a spectrophotometer (model Cary IE UV-Vis; Varian Inc., Palo Alto, CA, USA) for SOM_A quantification using a quartz cuvette and only solution without soil as the blank, according to Mikutta et al. (2007).

The SOM-A supernatant was filtered using a 0.22 μm pore size filter. The filtered liquid was then placed in 2 mL vials and dried completely in a vacuum concentrator without heating. Afterwards, the samples were derivatized in two steps, following the method described by López-González et al. (2023). The first step of the derivatization was methoximation, which involved adding 40 μL of methoxyamine hydrochloride (20 mg/mL in pyridine) to the dried samples and incubating them at 37 °C for 2 hours in a thermomixer set to 950 rpm. The second step of the derivatization was silylation, which involved adding 70 μL of MSTFA to the aliquots. The samples were then placed in a thermomixer at 37 °C and shaken for 30 min at 950 rpm. Finally, 110 μL of the derivatized samples were transferred to glass vials for GC-MS analysis (López-González et al., 2023).

The derivatized extracts were injected into a gas chromatograph apparatus (Thermo Fisher G-Trace 1310) coupled to a single quadrupole mass spectrometer (ISQ LT). Samples were chromatographically separated using a capillary column (TG-5MS 30 m × 0.25 mm × 0.25 μm), and helium (6.0) was used as the carrier gas. The injector and source were set at 250 °C and 260 °C, respectively. One μL of the sample was injected in splitless mode with a flow rate of 1 mL min$^{-1}$. The programmed temperature was set: an isothermal hold at 70 °C for 5 min, followed by a 5 °C min$^{-1}$ ramp to 350 °C with final heating at 330 °C for 5 min. Mass spectra were recorded in electronic impact (EI) mode at 70 eV, scanning in the 45–600 *m/z* range.

The MS-DIAL software, which has a publicly available EI spectra library, was used to extract, filter, and calibrate raw peaks. Additionally, it was used to align peaks, analyze deconvolution, integrate peak height, and annotate peaks. A peak width of 20 scans and a minimum amplitude of 1000 were used, with a sigma window value of 0.5 and EI spectra cut-off of 10 amplitudes for deconvolution. For peak identification,

retention time tolerance was set at 0.5 min, *m/z* tolerance was set at 0.5 Da, EI similarity cut-off was set at 70 %, and the identification score cut-off was set at 70 %. The alignment parameters and retention time tolerance were set at 0.075 min.

Publicly available libraries were used for compound annotation, based on mass spectral patterns compared to EI spectral libraries such as the MSRI spectral libraries from Golm Metabolome Database (Kopka et al., 2005) available from Max-Planck-Institute for Plant Physiology (Golm, Germany) and MassBank (Horai et al., 2010), MoNA (Mass Bank of North America). Once compounds and features were annotated and identified, shared metabolites were only reported as quantified and confidently identified. To identify metabolites, metabolomics standards initiative (MSI) guidelines for metabolite identification were followed (Fiehn et al., 2007). Samples were annotated at two levels: (i) Level 2, which involved identifying compounds based on a match factor greater than 70 % in the spectral database, and (ii) Level 3, which only allowed to identify compound groups based on specific ions and RT regions of metabolites (López-González et al., 2023).

### 2.6. Total bacterial counts

The total bacterial count was performed to characterize the soil bacterial load in response to the SOM-A availability, considering the different management practices. It was performed on an agar medium (tryptone 5.0 g $L^{-1}$, yeast extract 2.5 g $L^{-1}$, glucose 1.0 g $L^{-1}$, bacteriological agar 12.0 g $L^{-1}$ at pH 7.0 ± 0.2. This medium satisfies the requirements defined by ISO 4833 and the American Public Health Association (ISO, 4833, 2003). The prepared medium underwent an autoclave sterilization cycle at 121 °C for 20 min. An aliquot of 100 mg was suspended in 10 mL of distilled water for each soil sample and vortexed for 30 sec. After that, the other serial dilutions were prepared by progressively pipetting 1 mL of the previous dilution into 9 mL of distilled water, and the $10^{-4}$ and $10^{-5}$ dilutions were plated on agar Petri dishes (Ø = 90 mm). All plates were incubated at 37±2 °C for 48 h under aerobic conditions. After incubation, the colonies formed were counted with a stereomicroscope. The number of bacteria expressed in colony-forming units (CFU) was multiplied by the dilution factor to get the total CFU per gram of soil.

### 2.7. Statistical analysis

Statistical differences were evaluated, distinctly, on the aggregate abundance, the SOM-A content, and the bacterial count, in the univariate domain by three-way analyses of variance (three-way ANOVA), followed by Tukey post-hoc tests, considering three fixed variables: the aggregate size classes (>5, 5–2, 2–1, 1–0.250, 0.250–0.063, < 0.063 mm for the aggregate abundance; 1–0.250, 0.250–0.063, < 0.063 mm for the SOM content and the bacterial count), the typologies of treatments ($S_{mng}$ or $C_{mng}$) and the soil depth (0–5, 5–15, 15–30 cm). Whereas, in the multivariate domain, statistical differences, distinctly, on the STC, STN content, and C/N ratio and on mineralogical characteristics were evaluated through a multivariate analysis of variance (MANOVA), using the aggregate size classes, the typologies of treatments and the soil depth as fixed factors, with Pillai's trace (for STC, STN and C/N ratio) and Wilk's trace (for the mineral components) as the test statistics. A non-metric multidimensional scaling (NMDS), based on the Euclidean distance metric and on 2 axes, with the superimposition of confidence ellipses (α = 0.05) for treatments and soil depth for STC, STN and C/N ratio and the treatments and aggregate size classes for the mineralogy, was also subsequently performed. All the statistical and graphical analyses were conducted in the R 4.0.0 programming environment (R Core Team, 2020), with functions from the 'vegan', 'agricolae', 'dplyr', 'multcompView', 'ggplot2' and 'RColorBrewer' packages, and using the open-source vector graphics editor Inkscape 0.92.

Metabolomic data were analyzed using Metaboanalyst 5.0 (https://www.metaboanalyst.ca) (Pang et al., 2021). Three different comparisons were made for data analysis: (i) comparison according to agricultural practices ($C_{mng}$ *vs* $S_{mng}$), (ii) comparison according to depth (0–5 *vs* 5–15 *vs* 15–30 cm) and (iii) comparison according to granulometry (1–0.250 *vs* 0.250–0.063 *vs* < 0.063 mm). Metabolite concentrations were checked for accuracy, and any missing values were replaced with a small positive value (half of the minimum positive number detected in the data). The data were normalized, transformed through "Log normalization," and scaled using Pareto-Scaling. Unsupervised Principal Component Analysis (PCA) was used to create a score plot for group discrimination.

Further analysis was conducted through supervised partial least-squares discriminant analysis (PLS-DA) for depth and granulometry comparisons, and an ortho-PLS-DA was performed to compare agricultural practices. Features with the highest discriminatory power were selected based on their variable importance in the projection score. The PLS-DA and ortho-PLS-DA models were validated to avoid overfitting using Q2 as a performance measure, the 10-fold cross-validation and setting in the permutation test a permutation number of 20. Univariate analysis: one-way ANOVA was used to highlight statistical differences among single metabolites and treatments, with a false discovery rate applied to control for false-positive findings ($p \leq 0.05$) for depth and granulometry comparisons, and a t-test was used for agricultural practices comparison with a false discovery rate applied to control for false-positive findings ($p \leq 0.05$). Finally, all statistically significant features affected by the treatments were presented as a heatmap and clustered using the Euclidean method for distance measurement and the Ward algorithm for group clusterization.

## 3. Results and discussion

### 3.1. Aggregate size and C/N analyses

The aggregate distribution, determined by the dry weight percentage (% dw) for each aggregate size class (>5, 5–2, 2–1, 1–0.250, 0.250–0.063, < 0.063 mm), considering the typologies of treatments ($S_{mng}$ or $C_{mng}$) and the soil depth (0–5, 5–15, 15–30 cm), is reported in Fig. 1. The three-way ANOVA enabled the identification of highly significant differences in the aggregate distribution in relation to the aggregate size classes ($P < 0.001$). The macro-aggregates (with a diameter > 0.250 mm) in the 0–5 and 5–15 cm layers were more represented in the $S_{mng}$, while the opposite happened for micro-aggregates (with a diameter < 0.250 mm). This could be because of the less disturbance to the soil (no-till) and higher content of organic matter (see following data), acting as a cementing agent of soil particles (Rabbi et al., 2020). Indeed, it is known that the state of aggregation of soil particles is influenced by tillage performed in the $C_{mng}$, causing a disruption of macro-aggregates with a consequent increase of micro-aggregates (Grandy and Robertson, 2006; Olchin et al., 2008; Helgason et al., 2010). The higher abundance of large aggregates with a diameter >2 mm in the 15–30 cm of the $S_{mng}$ layer can depend on the difficulty that surface inputs of organic residues in the $S_{mng}$ had in reaching the deeper layers (Fig. 2a). Moreover, tillage in the $C_{mng}$ could also create a compacted soil sole underneath the tilled part (tillage sole), which may have induced the higher presence of of large macro-aggregates in this layer (Dimanche and Hoogmoed, 2002; Muruganandam et al., 2009; Addesso et al., 2023).

Fig. 2a shows the dry weight percentage of STC and STN, and C/N ratio, for each aggregate size class (1–0.250, 0.250–0.063, < 0.063 mm), considering the typologies of treatments ($S_{mng}$ or $C_{mng}$) and the soil depth (0–5, 5–15, 15–30 cm). Three-way MANOVA highlighted significant differences in relation to STC, STN content and C/N ratio, both among the two treatments (Pillai's trace = 0.909, $p \leq 0.001$) and the three different soil depths (Pillai's trace = 1.016, $p \leq 0.01$), but not among the aggregate size classes (Pillai's trace = 0.663, P=NS) (Supplementary Table S2). The NMDS (Fig. 2b), with superimposition of confidence ellipses for treatments and depths, showed differences

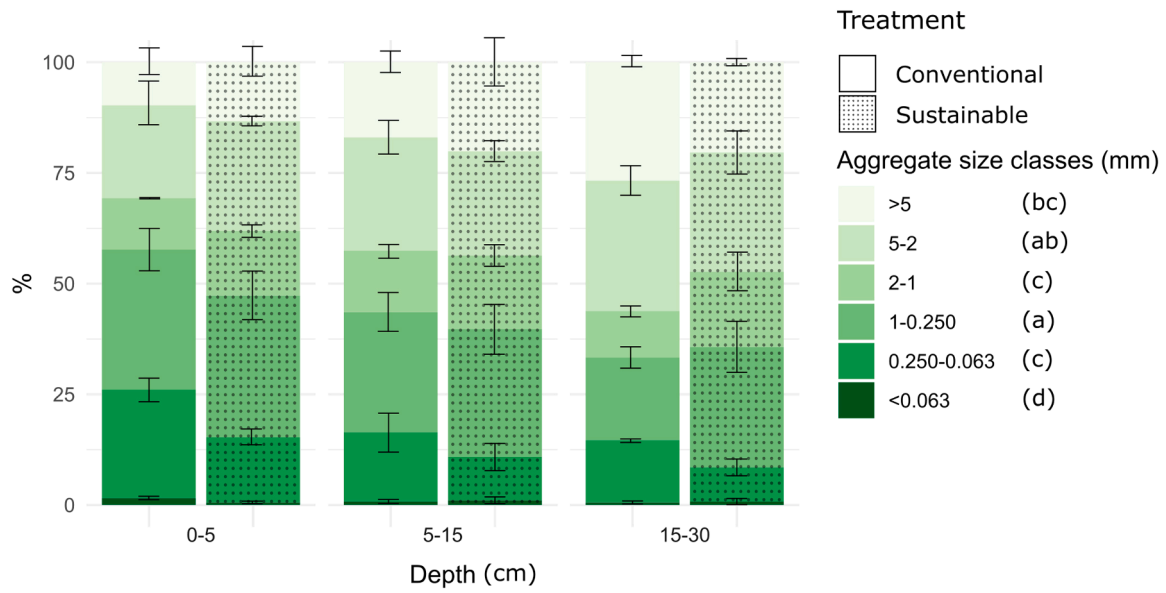


**Fig. 1.** Aggregate distribution, determined by the dry weight percentage (mean values) for each aggregate size class (>5, 5–2, 2–1, 1–0.250, 0.250–0.063, < 0.063 mm), based on the typologies of treatments ($S_{mng}$, $C_{mng}$) and the soil depth (0–5, 5–15, 15–30 cm). Range bars represent the standard deviations of the means. Different letters in the legend indicate significant differences (for $\alpha = 0.05$) among aggregate size classes, according to the Tukey post-hoc tests.

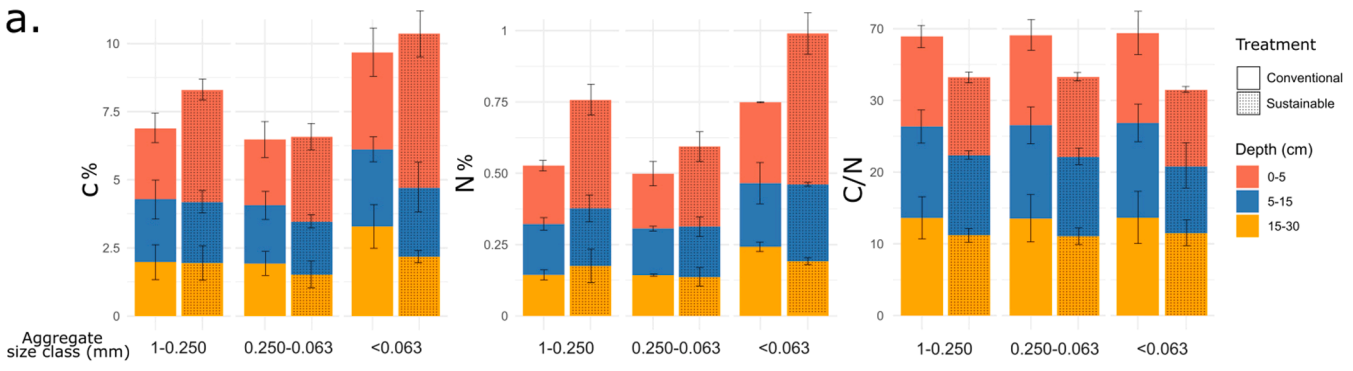


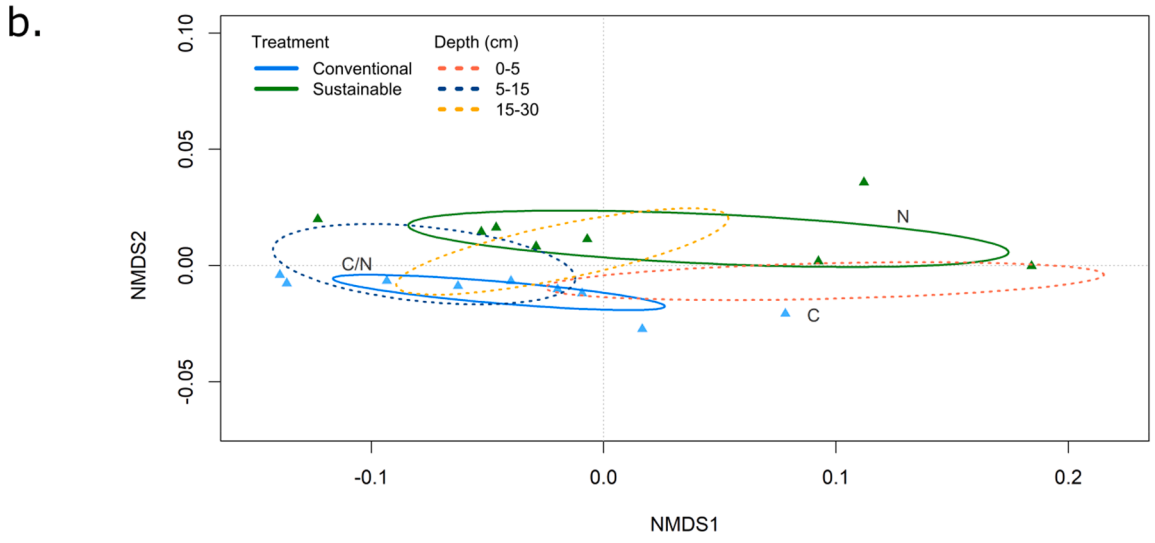


**Fig. 2. a)** Barplots showing the STC, STN content (% dw) and C/N ratio, for each aggregate size class (1–0.250, 0.250–0.063, < 0.063 mm), considering the typologies of treatments ($S_{mng}$, $C_{mng}$) and the soil depth (0–5, 5–15, 15–30 cm). Range bars represent the standard deviations of the means. **b)** NMDS biplot, with the superimposition of confidence ellipses for $\alpha = 0.05$, according to the typologies of treatments ($S_{mng}$, $C_{mng}$) and the soil depth (0–5, 5–15, 15–30 cm), based on STC, STN and C/N ratio values.

among the soil samples. In particular, it displayed a clear separation of the confidence ellipses grouping the $S_{mng}$ and $C_{mng}$ treatments, owing to the higher N and C concentrations in the $S_{mng}$, according to Wander and Traina (1996). Similarly, the soil sampled at 15–30 cm depth is clearly differentiated by that one sampled at 0–5 cm depth that showed a higher content of C and N (+50.7 % and +74.9 %, respectively), whereas that one sampled at 5–15 cm depth revealed intermediate characteristics, as highlighted by the partial overlapping of its confidence ellipse with the other two. The C/N ratio remained quite constant in the two cultivation systems in all samples, regardless of soil depth and aggregate size (Fig. 2a). The $S_{mng}$ showed a lower C/N ratio than the $C_{mng}$, due to the increase of STN (Fig. 2a).

The higher C and N amount in the soil surficial layer confirms that organic matter inputs in the $S_{mng}$ struggled to establish relationships with soil phases in the deeper layers (5–15 and 15–30 cm). It can also be hypothesized that STC and STN, and therefore also the SOM, increased in the < 0.063 mm aggregate class of the $S_{mng}$ (+59.3 % and +86.7 %, respectively), in accordance with Green et al. (2005), because they formed relationships more easily with particles having a smaller diameter, with a higher specific surface area, such as colloidal materials (Totsche et al., 2018).

### 3.2. XRPD mineralogical analysis

Fig. 3a reports the mineral assemblage of the studied soils, mainly consisting, in decreasing order of abundance, of quartz (qtz), plagioclase (albite-anorthite; plg), K-feldspar (with common orthoclase; ort), calcite (cal), and minor amounts of clay minerals (i.e., illite, montmorillonite, kaolinite and phlogophite), representing an assemblage typical of Basento valley (see the geological setting in the materials and methods section). Oxides occur in accessory phases. Three-way MANOVA highlighted significant differences in relation to the mineral composition of the samples, both among the two treatments (Wilks's trace = 0.056, $p \leq 0.001$) and the aggregate size classes (Wilks's trace = 0.028, $p \leq 0.01$), but not between the three different soil depths (Wilks's trace = 0.989, P = NS). The NMDS (Fig. 3b), with superimposition of confidence ellipses

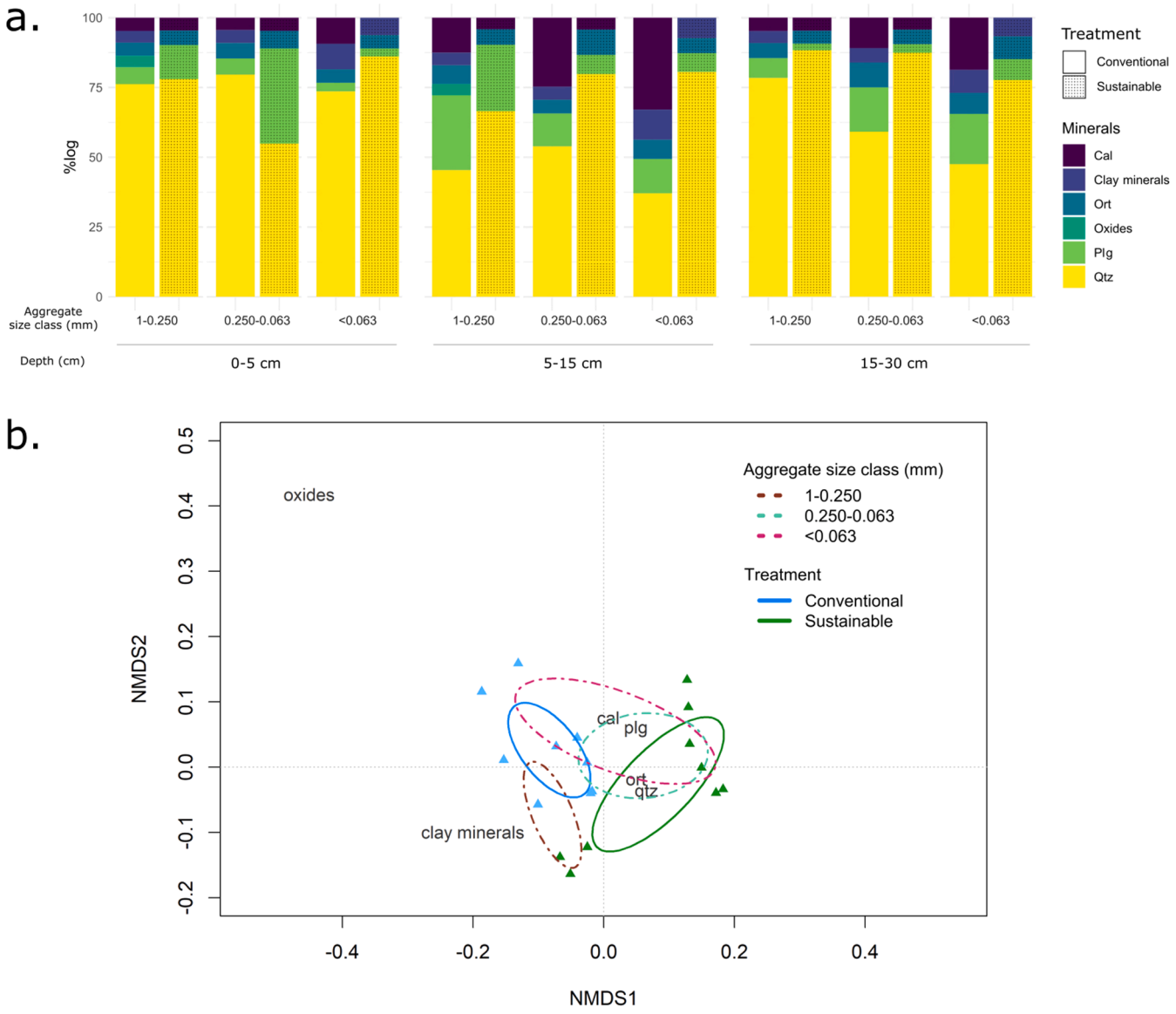


**Fig. 3. a)** Barplots showing the mineralogical composition of soil samples, considering the aggregate size classes (1–0.250, 0.250–0.063, < 0.063 mm), the typologies of treatments ($S_{mng}$, $C_{mng}$) and the soil depth (0–5, 5–15, 15–30 cm). For minerals, the following abbreviations were used: Cal - calcite, Qtz - quartz, Plg – plagioclase, Ort – orthoclase. **b)** NMDS biplot, with the superimposition of confidence ellipses for α = 0.05, according to the typologies of treatments ($S_{mng}$, $C_{mng}$) and the aggregate size class (1–0.250, 0.250–0.063, < 0.063 mm), based on the mineralogical composition of soil samples.

for treatments and aggregate size classes, highlighted a distinct separation among the confidence ellipses grouping the $S_{mng}$ and $C_{mng}$ treatments because of the higher qtz, plg, ort and cal content in the $S_{mng}$; similarly, 1–0.250 and 0.250–0.063 mm aggregate size classes are clearly differentiated by that one < 0.063 mm, showing also higher contents of qtz, plg, ort, and cal, whereas the < 0.063 mm class revealed a higher content of clay minerals than the other two size classes. The 1–0.250 mm class of $C_{mng}$ soils contained clastic minerals, such as qtz, plg, ort and cal. Furthermore, XRPD data highlighted various groups of phyllosilicate clays as by-products (secondary/pedogenic). In particular, 1:1 (i.e., kaolinite) and 2:1 clays (i.e., vermiculite and illite) are common weathering products of silicate minerals (White, 2005; Scarciglia et al., 2005; 2016). These latter include plg and ort, that were present in our soils (Fig. 3a).

Moreover, in the aggregate size class 0.250–0.063 mm of $C_{mng}$ soils, there were the same clastic minerals (qtz, plg, ort, cal) with clay minerals. As expected, in the class < 0.063 mm, there was a higher presence of phyllosilicate clay minerals besides the other clastic minerals (qtz, plg, ort, and cal). In the aggregate size classes 1–0.250 and 0.250–0.063 mm of $S_{mng}$ soils, clay minerals were not identified, but there were clastic minerals (qtz, plg, ort, and cal). Here, ort and plg showed a high crystallinity, probably because of a parent rock poorly weathered, given the absence of clay products. In < 0.063 mm class, referred to the $S_{mng}$, besides clastic mineral residues (qtz, plg, ort), there were also clay minerals (illite, kaolinite and montmorillonite), while cal was absent. Compared to $S_{mng}$ soils, $C_{mng}$ ones, in addition to qtz and plg, showed a higher content of cal and ort. In $C_{mng}$ soils, the presence of clastic minerals (cal and ort) was probably because of the clasts' breakage in the conglomerates following soil tillage and disturbance, while clay minerals derived from the alteration of plg and ort. In the same aggregate size classes, a higher crystallinity of clay minerals was noted in the $S_{mng}$ compared to the $C_{mng}$, likely because of its undisturbed cultivation. As all the studied soils derived from the same parent rock, likely a differential physical attack of the primary minerals could have influenced the newly formed components' quantification and the altered/non-altered ones in the different samples. Another explanation for the different mineral distribution between the two soil management types could be the reallocation of minerals across soil layers and aggregate classes caused by soil tillage disturbance occurring in the $C_{mng}$ (White, 2005).

### 3.3. FTIR analysis

Fig. 4 reports the spectra obtained through FTIR analysis, showing a similar general scheme, with seven main absorption bands at the following wave numbers (WN): (i) 1050 $cm^{-1}$ indicative for Si-O-Si groups in soil minerals (quartz, clay minerals), (ii) 1420 $cm^{-1}$ indicative for C═O bonds in SOM interacting with cations ($OM_{cat}$), (iii) 1650 $cm^{-1}$ indicative for $COO^-$ groups, (iv) 1720 $cm^{-1}$ indicative for COOH, (v) two small absorption bands at the shoulder of the broad OH band (WN 2700 and 2800 $cm^{-1}$) indicative for hydrophobic CH groups in SOM, and (vi) and a broad band at 3500 $cm^{-1}$, indicative for OH groups in SOM, adsorbed water, and soil minerals (Ellerbrock and Gerke, 2016). The band at WN 1050 $cm^{-1}$ was most intense because of the high content of soil minerals in the size fractions.

The spectra of all aggregate size classes of the $S_{mng}$ soil (Fig. 4a-c; left), considering the replicates I to III, showed slight differences in the intensity of the $OM_{cat}$ absorption band, indicative of SOM-cation/mineral interactions, which mostly decrease gradually in the sequence I > II > III, suggesting that the number of SOM-cation/-mineral interactions was higher in soils from replicate I as compared to those from replicates II or III. Whereas those related to $C_{mng}$ soils (Fig. 4a-c; right) showed superimposable band heights of the $OM_{cat}$, except for the replicate II, highlighting that the OM in these fractions is higher in the OM-cation associations amount, compared to both all $S_{mng}$ replicates and to the replicates I and III of the $C_{mng}$ fraction (Fig. 4a-c; red arrows). Such variabilities in SOM composition for the $S_{mng}$ and $C_{mng}$ treatments can result from soil management and tillage, which may create a different spatial heterogeneity (Vieublé-Gonod et al., 2009). The FTIR spectra of the < 0.063 mm fractions in $S_{mng}$ samples from different sampling depths showed that $OM_{cat}$ band intensities increased in the sequence 0–5 cm </= 5–15 cm < 15–30 cm, suggesting an increase of SOM-cation interactions with depth (Fig. 4d; left). The spectra of the $C_{mng}$ fractions did not show such differences (Fig. 4d; right). This can be likely explained, even in this case, by soil management type, which in the $C_{mng}$ included plowing up to 30-cm depth in the inter-row portion, with a consequent homogeneous distribution of soil components (Becher, 1995; Limousin and Tessier, 2007).

### 3.4. Quantitative and qualitative organic matter from aggregates (SOM-A) analysis

Like any soil constituent, organic matter, in its smaller and dissolved fractions, has relationships with the mineral phase of the soil, therefore it is stabilized within the aggregates. The soil mineral phase always absorbs substances circulating in the soil solution as it is characterized by surface charges (generally negative, changing with the soil pH), whose magnitude and selectivity depend on the type of mineral, the compound's nature, and the concentration in solution (Violante, 2013). Among the various compounds adsorbed by mineral colloids, there are organic molecules that are part of the dissolved organic matter (DOM) or that portion of organic matter dissolved in the soil solution.

Fig. 5 shows the absorbance values giving a quantitative indication of the SOM-A aromatic component content in the analyzed samples, considering each aggregate size class (1–0.250, 0.250–0.063, < 0.063 mm), the typologies of treatments ($S_{mng}$ or $C_{mng}$) and the soil depth (0–5, 5–15, 15–30 cm). The three-way ANOVA highlighted significant differences in SOM-A in relation to all the considered fixed variables among the typologies of treatments ($p \leq 0.001$), the three soil depths ($p \leq 0.001$) and among the aggregate size classes ($p \leq 0.01$). As for STC and STN, the SOM-A content in $S_{mng}$ soils was higher in the samples taken in the first few centimeters of soil (0–5 cm) (+ 76.0 %) with higher values in < 0.063 mm aggregates (+87.7 %) (Fig. 5a), and gradually decreasing in the other two layers (5–15 and 15–30 cm), with no significant differentiation. These results highlighted the impressive effects of soil management on SOM accumulation. Franzluebbers and Arshad (1997) found that soil organic carbon (SOC) increased of 10–30 % under no-tillage (NT) compared to conventional tillage (CT), with the consequent sequestration into SOC by biomass equal to 22 % under NT, versus only 9 % under CT. In $S_{mng}$ soils, the constant surficial cover and no tillage promoted the release and storage of organic matter with a continuous and fresh OM supply from surface, but it takes a long time before it establishes stable bonds with the soil mineral phases in the deeper layers (Komatsuzaki and Ohta, 2007). Moreover, the higher peak observed in the sustainable treatment at the finer particle size could be due to both the higher specific surface area of such fractions and the specific interactions established between the mineral phase and organic matter, which are usually much more abundant in the finer soil fraction (Sheehy et al., 2015; Totsche et al., 2018; Yeasmin et al., 2023).

SOM-A analyzed by GC-MS showed differences in results depending on the type of comparison. Based on the agricultural practices used, the PCA score plot was built using two components, PC1 *vs* PC2, and described 60.6 % of the total variability (Fig. 6a). PC1 explained the highest variance (49.6 %), while PC2 explained 11 % of the total variance. The PCA revealed discrimination between the groups, but the separation was unclear. The supervised ortho-PLS-DA showed a clear separation between the $S_{mng}$ and the $C_{mng}$. The separation was achieved by the first two principal components (orthogonal T score *vs* T score), which explained a total variance of 50.7 %. The orthogonal T score explained the highest variance (27.3 %), while the T score explained 23.4 % of the total variance (Fig. 6b). The variable importance of projection (VIP) scores derived from the ortho-PLS-DA analysis

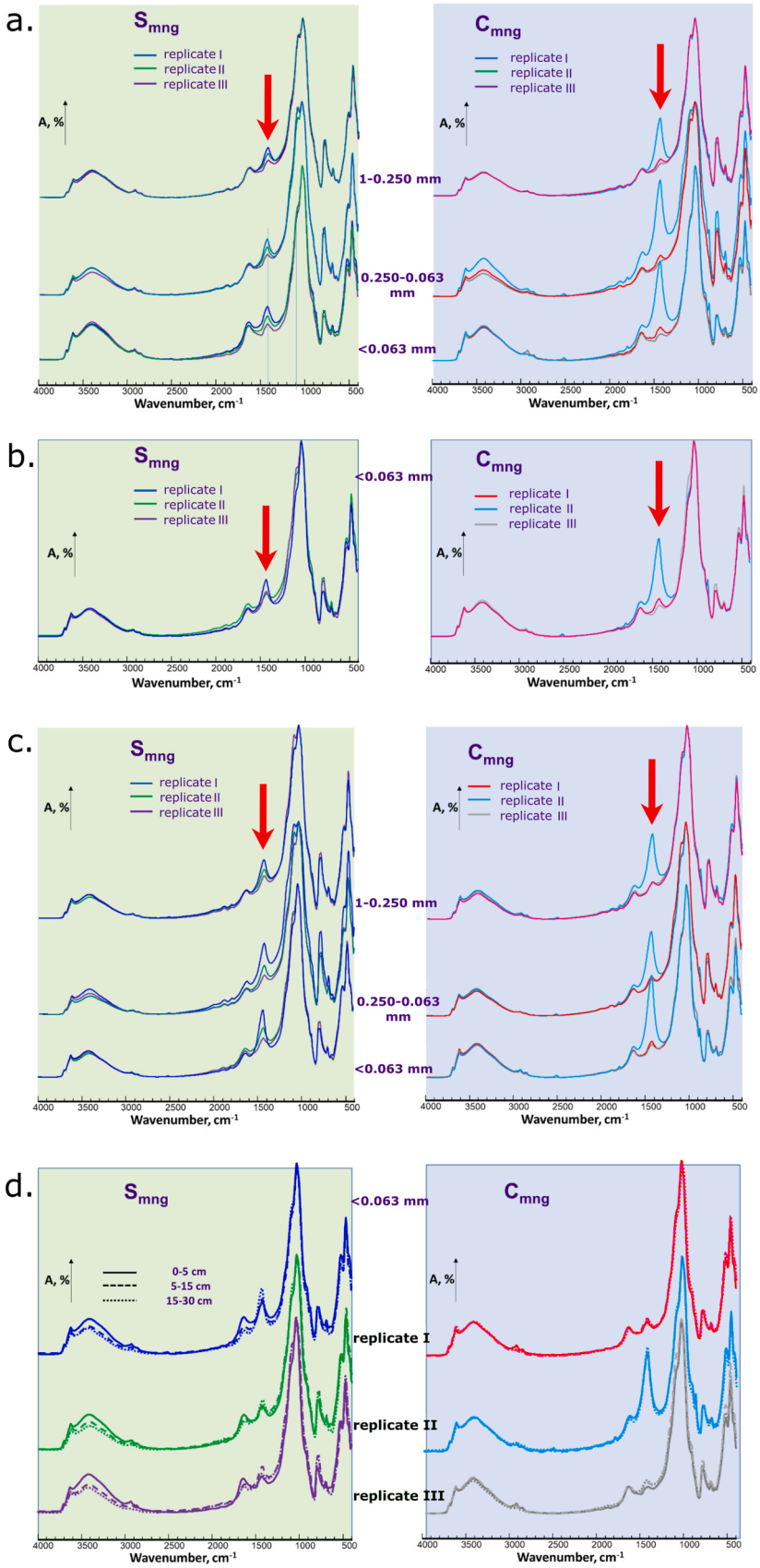


**Fig. 4.** FTIR spectra of **(a)** 1–0.250 mm, 0.250–0.063 mm and < 0.063 mm sized fractions. **(b)** FTIR spectra of < 0.063 mm sized fraction, both collected at 0–5 cm depth from $S_{mng}$ (left) and $C_{mng}$ (right) soils. **(c)** FTIR spectra of 1–0.250 mm, 0.250–0.063 mm and < 0.063 mm collected at 15–30 cm depth from $S_{mng}$ (left) and $C_{mng}$ (right) soils. **(d)** FTIR spectra of < 0.063 mm sized fraction collected at 0–5 cm, 5–15 cm and 15–30 cm depths from $S_{mng}$ (left) and $C_{mng}$ (right) soils.

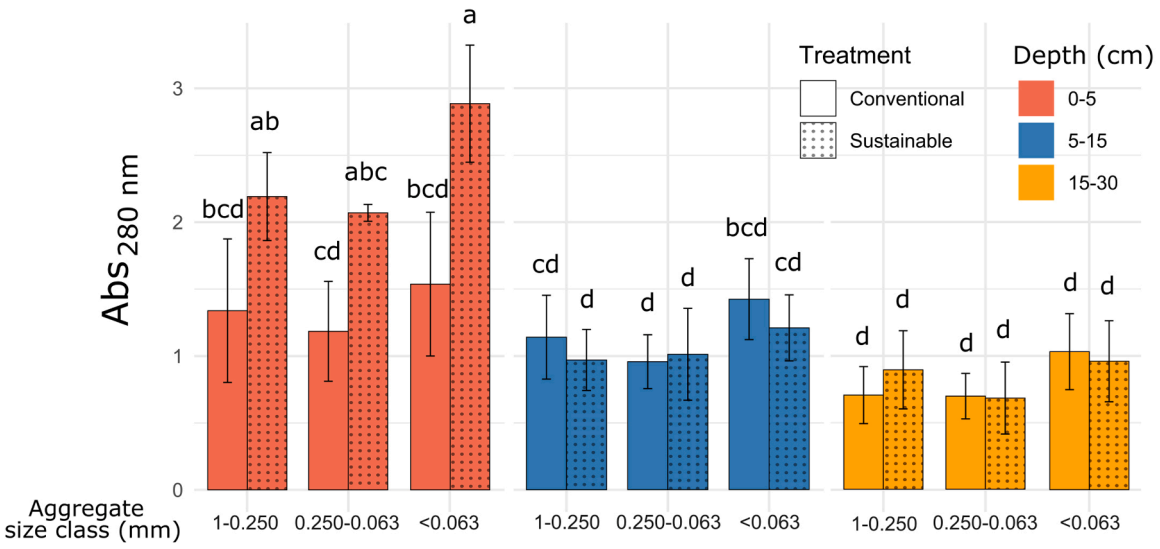


**Fig. 5.** Organic matter from aggregates (SOM-A) content of soil samples for each aggregate size class (1–0.250, 0.250–0.063, < 0.063 mm), considering the typologies of treatments ($S_{mng}$, $C_{mng}$) and the soil depth (0–5, 5–15, 15–30 cm). Range bars represent the standard deviations of the means.

(constructed based on metabolites with a VIP score greater than 1.4) showed that certain metabolites, including D-(+)-galactose, behenic acid, 4-hydroxybutyric acid, urea, icosanoic acid, stearic acid, 4-hydroxypyridine, oleic acid, and L-pyroglutamic acid, were the primary contributors to the differentiation between the groups (Fig. 6c). A t-test was performed to find which metabolites were significantly altered among treatments (López-González et al., 2023). The analysis revealed that 34 out of the 56 compounds identified were significantly altered. Those metabolites were presented on a heatmap showing how each metabolite varied according to the management (Fig. 6d).

In the $C_{mng}$, an accumulation of some amino acids (β-alanine, L-alanine, and L-valine), polyamines (e.g., putrescine); some sugars (β-D-glucose, D-arabinose, and D-galactose), as well as urea, was observed, while these were reduced in the $S_{mng}$. In the $S_{mng}$, an accumulation of fatty acids (palmitic acid, stearic acid, oleic acid, myristic acid and heptadecanoic acid), organic acids (salicylic acid, behenic acid, icosanoic acid, fumaric acid, gallic acid, and others), and sugars (e.g., D-ribose), which were reduced in the $C_{mng}$, was recorded. The accumulation of organic acids and short-chain fatty acids, as observed in the $S_{mng}$, is common in soils characterized by fermentative soil microbes (Melero et al., 2006; Jonhs et al., 2017).

Concerning the depth comparison, as in the comparison of farming practices, the PCA score plot was built using two components, PC1 *vs* PC2, and described 60.6 % of the total variability (Fig. 7a). PC1 explained the highest variance (49.6 %), while PC2 explained 11 % of the total variance. The PCA revealed discrimination between the groups, but the separation is much more unclear than with the comparison of agricultural practices. Here, the supervised PLS-DA showed an unclear separation among the depths analyzed, with a small separation of the 0–5 cm depth from the other two depths. The separation was achieved by the first two principal components (component 1 *vs* component 2), which explained a total variance of 53.3 %. Component 1 explained the highest variance (49.2 %), while component 2 explained 4.1 % of the total variance (Fig. 7b). The VIP scores derived from the PLS-DA analysis showed β-D-(+)-glucose, 2-furoic acid, D-(−)-arabinose, L-alanine, 1–3-diaminopropane, oleic acid, stearic acid, and icosanoic acid, were the metabolites that mainly contributed to the differentiation among the depths (Fig. 7c).

A univariate ANOVA was performed to reveal which metabolites were significantly altered among treatments. As a result, 27 out of the 56 compounds identified were significantly altered. Those metabolites were presented on a heatmap showing how each metabolite varied according to the depth group (Fig. 7d). The 0–5 cm depth was characterized by an increased accumulation of organic acids (2-furoic acid, 3-hydroxybenzoic acid, 4-hydroxybenzoic acid, behenic acid, fumaric acid, icosanoic acid, and succinic acid) and some fatty acids (heptadecanic acid, nonadecylic acid, myristic acid, oleic acid, palmitic acid, and stearic acid) which were reduced at the soil depths 5–15 and 15–30 cm. These latter accumulated amino acids (valine and alanine), sugars (D-arabinose and β-D-glucose), and other compounds (urea, 4-hydroxybutyric acid, 1–3 diaminopropane and dithiothreitol), which were reduced at the 0–5 cm depth. The richness of metabolites observed in the top layers is common in various soils, as microbial activity generates the appearance of different metabolites, causing the amount of SOM-A to be higher in more superficial layers than in deeper layers (Roth et al., 2019). The ANOVA confirmed the trend observed in the PLS-DA, whereby the 0–5 cm depth differed from the other two depths. Sucrose was a special case because it did not vary at the 0–5 cm depth, while it was accumulated at the 5–15 cm depth, and decreased at the 15–30 cm depth.

Finally, in the comparison based on granulometry, the PCA constructed using two components (PC1 *vs* PC2), described 60.6 % of the total variability as in the previous cases (PC1 explained the 49.6 %, while PC2 explained 11 % of the total variance; Fig. 8a). The supervised PLS-DA did not show a clear separation among the aggregate size classes. The separation was achieved by the first two principal components (component 1 *vs* component 2), which explained a total variance of 53.6 %. Component 1 explained the highest variance (47.7 %), while component 2 explained 5.9 % of the total variance (Fig. 8b). The VIP scores derived from the PLS-DA analysis indicated that 2-furoic acid, hydroxycarbamate, hydroxybutyric acid, 3-hydroxybenzoic acid, putrescine, L-valine, oleic acid, myristic acid, stearic acid, heptadecanic acid, and behenic acid were the main contributors to the separation among the aggregate size classes (Fig. 8c). Unlike the other two comparisons based on agronomic management and soil depth, the ANOVA performed in this comparison did not show any significantly altered metabolites.

The organic matter dissolved in the soil solution is generally composed of strongly decomposed organic fractions, such as protein residues and low-molecular-weight organic acids that can have cationic or anionic behavior by interacting with the colloidal phase of the soil. Organic molecules with cationic behavior can be easily adsorbed onto negatively charged colloids. Although large and therefore low in charge density, these molecules are retained on negative surfaces and can be

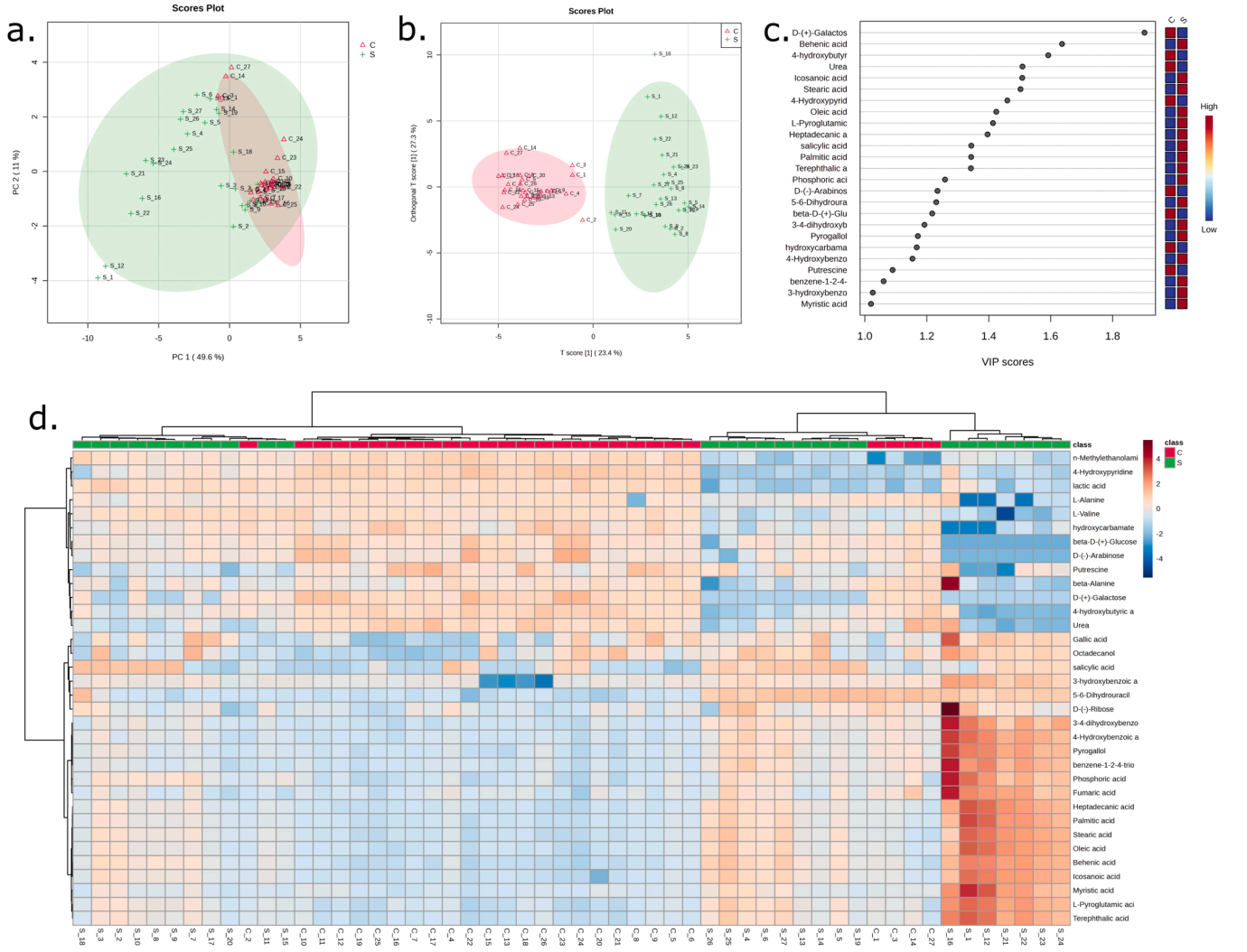


**Fig. 6.** **(a)** Unsupervised PCA of the metabolomic changes comparing $S_{mng}$ (S) and $C_{mng}$ (C). **(b)** Ortho-PLS-DA analysis of the metabolomic changes comparing $S_{mng}$ (S) and $C_{mng}$ (C). **(c)** Important features identified by ortho-PLS-DA. The colored boxes on the right indicate the relative concentrations of the corresponding metabolite in each group under study. **(d)** The clustering result is shown as a heatmap (distance measure using Euclidean and clustering algorithm using Ward method) of all the metabolites identified comparing $S_{mng}$ (S) and $C_{mng}$ (C). Each square represents the effect of the type of management on the amount of each metabolite using a false-color scale. Red or blue regions indicate increased or decreased metabolite content, respectively.

exchanged for more related ions. For example, among these molecules are most of those containing amine groups, which protonate to form an R-$NH_3^+$ complex. By forming this group, various proteins and enzymes can be adsorbed into the interlayers of expandable minerals, thus being sterically protected and less susceptible to degradation (Sequi, 2017).

### 3.5. Microbiological activity

Soils provide a habitat for many bacterial communities that influence soil fertility and plant growth by regulating nutrient availability and turnover (Borken et al., 2002). Microbial populations (bacterial and fungal) are the entities responsible for degrading all organic compounds in the soil. In response to different management practices, changes in the structure and dynamics of soil microbial communities can provide the basis for an index of soil health and fertility (Ding et al., 2013). Consequently, monitoring their quantity in the various samples becomes essential, analysing them differentially according to management techniques and then in relation to the other parameters. Fig. 9 shows the total bacterial counts in the analyzed samples. In all graphs, the standard deviation values were high, which can be explained because the values come from averages calculated on samples taken from different locations; consequently, they fall within the normal heterogeneity of the soil. The three-way ANOVA highlighted significant differences in bacterial counts in relation to all the considered fixed variables, among the typologies of treatments ($p \leq 0.05$), the three soil depths ($p \leq 0.01$) and among the aggregate size classes ($p \leq 0.01$), with the higher values generally found in the $S_{mng}$. This is in accordance with several studies comparing the microbiological activity in sustainably and conventionally managed soils (Maeder et al., 2002; Van Diepeningen et al., 2006; Liu et al., 2007; Baiano et al., 2024). In the $S_{mng}$, the highest bacterial number was always found in the smallest size class at all soil depths (Fig. 9). Regarding the trend of the $C_{mng}$, while up to 15 cm depth there was a trend similar to that found in the $S_{mng}$ (highest bacterial number in the finest particles), in the layer 15–30 cm a reversal was denoted. Here, counts were higher in the largest particle size class (1–0.250 mm), likely because the mineral nutrients added to the soil could diffuse up to

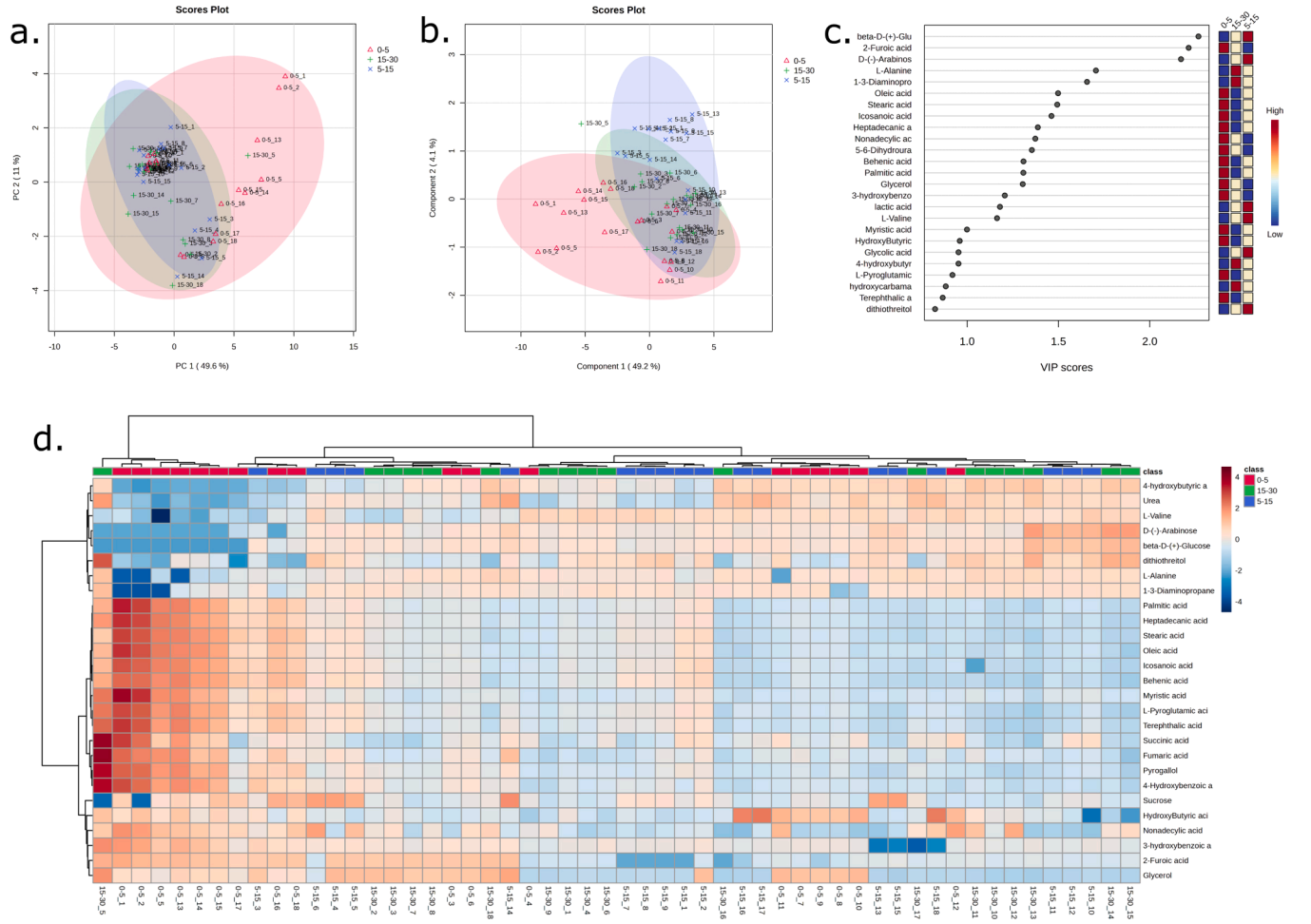


**Fig. 7.** **(a)** Unsupervised PCA of the metabolomic changes comparing the different depths tested (0–5, 5–15, 15–30 cm). **(b)** PLS-DA analysis of the metabolomic changes comparing the different depths tested. **(c)** Important features identified by PLS-DA. The colored boxes on the right indicate the relative concentrations of the corresponding metabolite in each group under study. **(d)** The clustering result is shown as a heatmap (distance measure using Euclidean and clustering algorithm using Ward method) of all the metabolites identified, comparing the different depths tested. Each square represents the effect of the depth on the amount of each metabolite using a false-color scale. Red or blue regions indicate increased or decreased metabolite content, respectively.

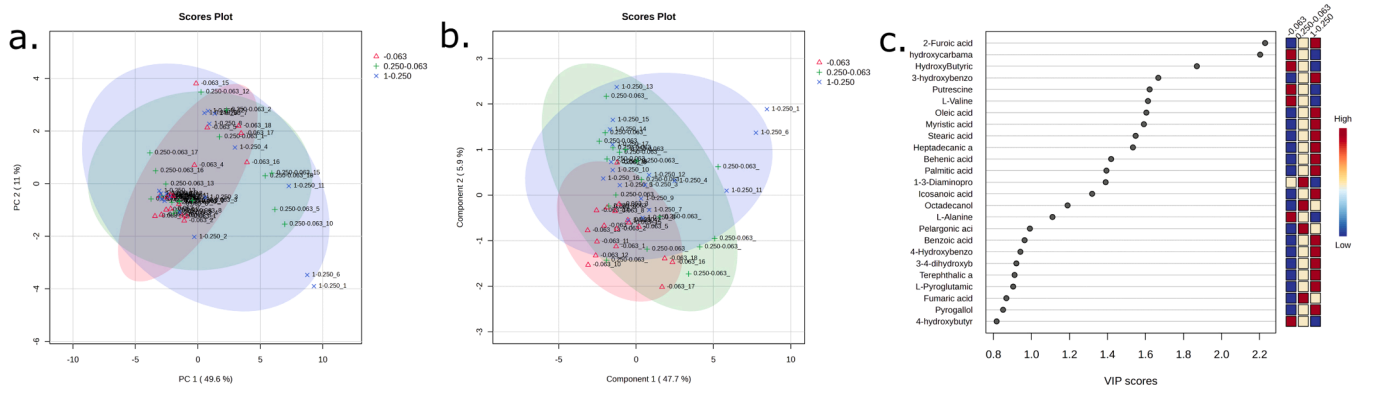


**Fig. 8.** **(a)** Unsupervised PCA of the metabolomic changes comparing the different particle sizes analysed (1–0.250, 0.250–0.063, < 0.063 mm). **(b)** PLS-DA analysis of the metabolomic changes comparing the different particle sizes analysed. **(c)** Important features identified by PLS-DA. The colored boxes on the right indicate the relative concentrations of the corresponding metabolite in each group under study.

30 cm, especially if bound to the larger soil particles.

Regarding the depths, the results of STC, STN, and SOM-A were also confirmed from a microbiological point of view. In fact, a lower bacterial number was found where there was a lower amount of STC, STN, and SOM-A, particularly at 15–30 cm depth. These results can be related to the fact that the soil was poorer in essential nutrients and, therefore, not entirely supportive of bacterial growth. Considering the trend among the particle size classes, a significant increase in the difference between the two management systems was found in the smaller fraction (< 0.063 mm). This result correlated with those obtained for STC and STN

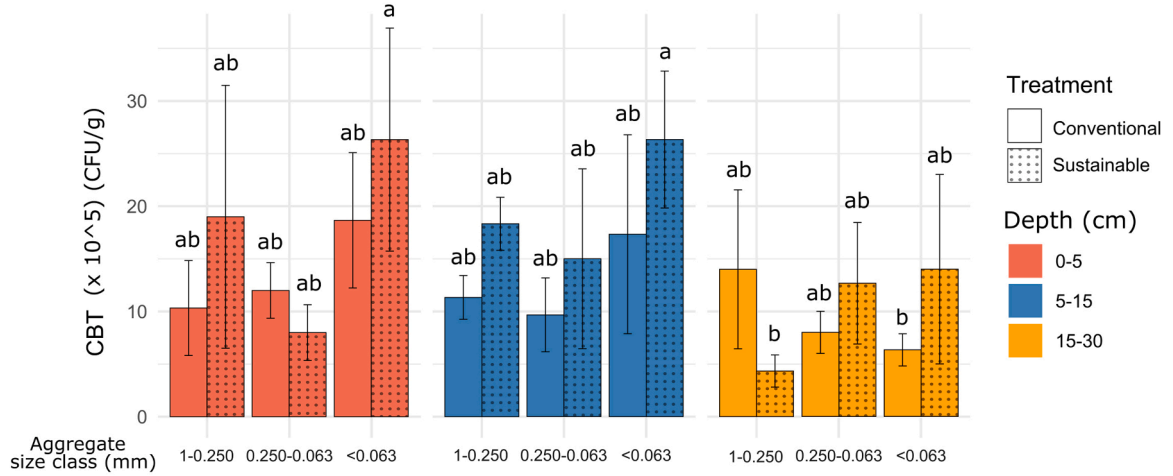


**Fig. 9.** Total bacterial counts in soil samples, considering the aggregate size classes (1–0.250, 0.250–0.063, < 0.063 mm), the typologies of treatments ($S_{mng}$, $C_{mng}$) and the soil depth (0–5, 5–15, 15–30 cm). Range bars represent the standard deviations of the means.

analyses, indicating that both organic C and N were more retained by the smaller aggregates and, consequently, the microbiological phase of the soil grew in these fractions.

## 4. Conclusions

This study highlighted that distinguishing SOM quantity, quality, and interaction with mineral components can help to understand if the potential for desorption of SOM determines its degradability and the dynamics of carbon accumulation into the soil, both essential for mitigating the effects of climate change, promoting land protection and increasing agricultural yields. Indeed, the continued adoption of conventional practices inevitably led to a gradual depletion of SOM. The positive effects related to sustainable practices were clearer in the topsoil (0–5 cm). This was likely because surface organic matter inputs struggled to seep the deeper profiles, especially in the absence of soil tillage. It is therefore clear that soil chemical and physical changes caused by a sustainable management occur relatively slowly. This also means that there must be an urgent turn in the management of Mediterranean agricultural sites in order to have the contrast and buffer the soil degradative processes that will happen in the future.

As a final suggestion, in order to maximize soil health in Mediterranean orchards, living roots should be maintained, i.e., the soil needs to be covered in a mantle of diverse living plants (cover crops or spontaneous weeds) for as long as possible, while bare soil should be avoided. Besides living plants and their root exudates, plant residues (e.g., stalks and leaves) and compost can also drive soil health. The benefits of a sustainable soil management are not merely productive, but they also include environmental, social and ethical aspects. This is a prerequisite for trying to maintain the functional autonomy of orchard agroecosystems over time and ensuring that they continue to perform their wide range of ecosystem services.

## Funding

This study was carried out within the Agritech National Research Center and received funding from the European Union NextGenerationEU (Piano Nazionale di Ripresa e Resilienza (PNRR) – missione 4, componente 2, investimento 1.4 – D.D. 1032 17/06/2022, CN00000022). This manuscript reflects only the authors' views and opinions, neither the European Union nor the European Commission can be considered responsible for them.

A part of this research was supported by the German Academic Exchange Service (DAAD) Research Stay titled 'Distinguishing soil organic matter quantity and quality from differently managed agricultural soils', carried out by Adriano Sofo at the Center for Environmental Research and Sustainable Technology (UFT), University of Bremen, Germany (Funding program/-ID: Research Stays for University Academics and Scientists, 2021, no. 57552334).

This study was partially funded by the national research program PRIN (Research Projects of Significant National Interest) in the frame of the project PRIN2017 "Emerging contaminants and reuse of treated wastewater in agriculture: fate in soil and plant system, ecophysiological response, soil microbiota and antibiotic resistance", Prot. 2017C5CLFB.

## CRediT authorship contribution statement

**Juliane Filser:** Supervision. **Domenico Sileo:** Methodology. **Rosangela Addesso:** Writing – review & editing, Methodology, Formal analysis, Data curation. **Adriano Sofo:** Writing – review & editing, Supervision, Project administration, Methodology, Funding acquisition, Data curation, Conceptualization. **Fabrizio Araniti:** Writing – review & editing, Methodology, Formal analysis, Data curation. **David Lopez-Gonzalez:** Writing – review & editing, Methodology, Formal analysis, Data curation. **Hazem S. Elshafie:** Writing – review & editing, Methodology, Formal analysis. **Ruth H. Ellerbrock:** Supervision. **Laura S. Schnee:** Writing – review & editing, Conceptualization. **Andrea Bloise:** Writing – review & editing, Methodology, Formal analysis, Data curation. **Alba N. Mininni:** Writing – review & editing, Methodology, Formal analysis, Data curation. **Bartolomeo Dichio:** Writing – review & editing, Funding acquisition, Conceptualization.

## Declaration of Competing Interest

The authors declare the following financial interests/personal relationships which may be considered as potential competing interests: Adriano Sofo reports financial support was provided by German Academic Exchange Service (DAAD). If there are other authors, they declare that they have no known competing financial interests or personal relationships that could have appeared to influence the work reported in this paper.

## Acknowledgments

The authors would like to thank Prof. Angela Ostuni of the University of Basilicata for making her laboratory available.

## Appendix A. Supporting information

Supplementary data associated with this article can be found in the

online version at doi:10.1016/j.agee.2024.109388.

## Data availability

Data will be made available on request.

## References


Addesso, R., De Waele, J., Cafaro, S., Baldantoni, D., 2022. Geochemical characterization of clastic sediments sheds light on energy sources and on alleged anthropogenic impacts in cave ecosystems. Int. J. Earth Sci. 111 (3), 919–927. https://doi.org/10.1007/s00531-021-02158-x.

Addesso, R., Morozzi, P., Tositti, L., De Waele, J., Baldantoni, D., 2023. Dripping and underground river waters shed light on the ecohydrology of a show cave. Ecohydrology 16 (3), e2511. https://doi.org/10.1002/eco.2511.

Alvarez-Puebla, R.A., Garrido, J.J., Valenzuela-Calahorro, C., Goulet, P.J.G., 2005. Retention and induced aggregation of Co(II) on a humic substance: sorption isotherms, infrared absorption, and molecular modeling. Surf. Sci. 575, 136–146.

Baiano, S., Picariello, E., Canfora, L., Tittarelli, F., Morra, L., 2024. Different organic farming systems under greenhouse do not improve soil C storage but affect microbial functions across soil aggregates. Soil Use Manag. 40 (1), e13011. https://doi.org/10.1111/sum.13011.

Becher, H.H., 1995. On the importance of soil homogeneity when evaluating field trials. J. Agron. Crop Sci. 174, 33–40. https://doi.org/10.1111/j.1439-037X.1995.tb00192.x.

Benitez, E., Nogales, R., Campos, M., Ruano, F., 2006. Biochemical variability of olive-orchard soils under different management systems. Appl. Soil Ecol. 32, 221–231. https://doi.org/10.1016/j.apsoil.2005.06.002.

Bentivenga, M., Coltorti, M., Prosser, G., Tavarnelli, E., 2004. A new interpretation of terraces in the Taranto Gulf: the role of extensional faulting. Geomorphology 60, 383–402. https://doi.org/10.1016/j.geomorph.2003.10.002.

Borken, W., Muhs, A., Beese, F., 2002. Changes in microbial and soil properties following compost treatment of degraded temperate forest soils. Soil Biol. Biochem. 34, 403–412.

Canisares, L.P., Banet, T., Rinehart, B., McNear, D., Poffenbarger, H., 2023. Litter quality and living roots affected the formation of new mineral-associated organic carbon but did not affect total mineral-associated organic carbon in a short-term incubation. Geoderma 430, 116302. https://doi.org/10.1016/j.geoderma.2022.116302.

Celi, L., Schnitzer, M., Nègre, M., 1997. Analysis of carboxyl groups in soil humic acids by a wet chemical method, Fourier-transform infrared spectrophotometry, and solution-state carbon-13 nuclear magnetic resonance. A comparative study. Soil Sci. 162 (3), 189–197.

Chittora, D., Meena, M., Barupal, T., Swapnil, P., Sharma, K., 2020. Cyanobacteria as a source of biofertilizers for sustainable agriculture. Biochem. Biophys. Rep. 22, 100737. https://doi.org/10.1016/j.bbrep.2020.100737.

Dimanche, P.-H., Hoogmoed, W.B., 2002. Soil tillage and water infiltration in semi-arid Morocco: the role of surface and sub-surface soil conditions. Soil Tillage Res. 66, 13–21. https://doi.org/10.1016/S0167-1987(02)00006-5.

Ding, G.C., Piceno, Y.M., Heuer, H., Weinert, N., Dohrmann, A.B., Carrillo, A., Andersen, G.L., Castellanos, T., Tebbe, C.C., Smalla, K., 2013. Changes of soil bacterial diversity as a consequence of agricultural land use in a semi-arid ecosystem. PLOS One 8, e59497.

Doran, J.W., Parkin, T.B., 1994. 1 Defining and assessing soil quality for a sustainable environment. Special. Publication 35. American Society of. Agronomy, Madison, Wisconsin, pp. 3–21.

Doran, J.W., Zeiss, M.R., 2000. Soil health and sustainability: managing the biotic component of soil quality. Appl. Soil Ecol. 15, 3–11. https://doi.org/10.1016/S0929-1393(00)00067-6.

Ellerbrock, R.H., Gerke, H.H., 2013. Characterization of organic matter composition of soil and flow path surfaces based on physicochemical principles—a review. Advances in Agronomy. Elsevier, pp. 117–177. https://doi.org/10.1016/B978-0-12-407685-3.00003-7.

Ellerbrock, R.H., Gerke, H.H., 2016. Analyzing management-induced dynamics of soluble organic matter composition in soils from long-term field experiments. Vadose Zone J. 15, vzj2015.05.0074. https://doi.org/10.2136/vzj2015.05.0074.

Ellerbrock, R.H., Höhn, A., Rogasik, J., 1999. Functional analysis of soil organic matter with respect to soil management. Eur. J. Soil Sci. 50, 65–71.

Fiehn, O., Robertson, D., Griffin, J., Vab Der Werf, M., Nikolau, B., Morrison, N., Sumner, L.W., Goodacre, R., Hardy, N.W., Taylor, C., et al., 2007. The metabolomics standards initiative (MSI). Metabolomics 3, 175–178.

Fierer, N., Wood, S.A., Bueno De Mesquita, C.P., 2021. How microbes can, and cannot, be used to assess soil health. Soil Biol. Biochem. 153, 108111. https://doi.org/10.1016/j.soilbio.2020.108111.

Franzluebbers, A.J., Arshad, M.A., 1997. Particulate organic carbon content and potential mineralization as affected by tillage and texture. Soil Sci. Soc. Am. J. 61 (5), 1382–1386. https://doi.org/10.2136/sssaj1997.03615995006100050014x.

Gonçalves, A.L., 2021. The use of microalgae and cyanobacteria in the improvement of agricultural practices: a review on their biofertilising, biostimulating and biopesticide roles. Appl. Sci. 11 (2), 871. https://doi.org/10.3390/app11020871.

González-Pérez, J.A., González-Vila, F.J., Ball, A.S., 2005. Soil health—a new challenge. Int. Microbiol. 8, 13–21.

Grandy, A.S., Robertson, G.P., 2006. Aggregation and organic matter protection following tillage of a previously uncultivated soil. Soil Sci. Soc. Am. J. 70, 1398–1406. https://doi.org/10.2136/sssaj2005.0313.

Green, V.S., Cavigelli, M.A., Dao, T.H., Flanagan, D.C., 2005. Soil physical properties and aggregate-associated C, N, and P distributions in organic and conventional cropping systems. Soil Sci. 170 (10), 822–831. https://doi.org/10.1097/01.ss.0000190509.18428.fe.

Gualtieri, A.F., Gatta, G.D., Arletti, R., Artioli, G., Ballirano, P., Cruciani, G., Guagliardi, A., Malferrari, D., Masciocchi, N., Scardi, P., 2019. Quantitative phase analysis using the Rietveld method: towards a procedure for checking the reliability and quality of the results. Period. Mineral. 88, 147–151, 2019.

Guimarães, D.V., Gonzaga, M.I.S., Da Silva, T.O., Da Silva, T.L., Da Silva Dias, N., Matias, M.I.S., 2013. Soil organic matter pools and carbon fractions in soil under different land uses. Soil Tillage Res. 126, 177–182. https://doi.org/10.1016/j.still.2012.07.010.

Haberhauer, G., Gerzabek, M.H., 1999. DRIFT and transmission FT-IR spectroscopy of forest soils: an approach to determine decomposition processes of forest litter. Vibr. Spectrosc. 19/2, 415-415.

Haghighi, F., Gorji, M., Shorafa, M., 2010. A study of the effects of land use changes on soil physical properties and organic matter. Land Degrad. Dev. 21 (5), 496–502, 10.1002/ldr.999.

Helgason, B.L., Walley, F.L., Germida, J.J., 2010. No-till soil management increases microbial biomass and alters community profiles in soil aggregates. Appl. Soil Ecol. 46, 390–397. https://doi.org/10.1016/j.apsoil.2010.10.002.

Horai, H., Arita, M., Kanaya, S., Nihei, Y., Ikeda, T., Suwa, K., Ojima, Y., Tanaka, K., Tanaka, S., Aoshima, K., et al., 2010. MassBank: a public repository for sharing mass spectral data for life sciences. J. Mass Spectrom. 45, 703–714.

Iglesias, A., Garrote, L., Flores, F., Moneo, M., 2007. Challenges to manage the risk of water scarcity and climate change in the Mediterranean. Water Resour. Manag. 21, 775–788. https://doi.org/10.1007/s11269-006-9111-6.

ISO 4833, 2003. Microbiology of food and animal feeing stuffs – Horizontal method for the enumeration of microorganisms – Colony count technique at 30 °C.

Kalyanasundaram, G.T., Ramasamy, A., Rakesh, S., Subburamu, K., 2020. Microalgae and cyanobacteria: role and applications inagriculture. Applied Algal Biotechnology. Nova Science Publishers, Hauppauge, NY, USA. ISBN 978-1-53617-524-0.

Kane, D.A., Bradford, M.A., Fuller, E., Oldfield, E.E., Wood, S.A., 2021. Soil organic matter protects US maize yields and lowers crop insurance payouts under drought. Environ. Res. Lett. 16, 044018. https://doi.org/10.1088/1748-9326/abe492.

Keesstra, S., Pereira, P., Novara, A., Brevik, E.C., Azorin-Molina, C., Parras-Alcántara, L., Jordán, A., Cerdà, A., 2016. Effects of soil management techniques on soil water erosion in apricot orchards. Sci. Total Environ. 551–552, 357–366. https://doi.org/10.1016/j.scitotenv.2016.01.182.

Komatsuzaki, M., Ohta, H., 2007. Soil management practices for sustainable agro-ecosystems. Sustain. Sci. 2 (1), 103–120. https://doi.org/10.1007/s11625-006-0014-5.

Kopka, J., Schauer, N., Krueger, S., Birkemeyer, C., Usadel, B., Bergmuller, E., Dormann, P., Weckwerth, W., Gibon, Y., Stitt, M., Willmitzer, L., Fernie, A.R., Steinhauser, D., 2005. GMD@CSB.DB: the Golm metabolome database. Bioinformatics 21, 1635–1638. https://doi.org/10.1093/bioinformatics/bti236.

Lal, R., 2017. World Reference Base for Soil Resources. Encyclopedia of Soil Science, Third Edition. Taylor & Francis Group, Abingdon-on-Thames, Oxfordshire United Kingdom.

Leifeld, J., Kögel-Knabner, I., 2005. Soil organic matter fractions as early indicators for carbon stock changes under different land-use? Geoderma 124 (1–2), 143–155. https://doi.org/10.1016/j.geoderma.2004.04.009.

Li, X., Yang, T., Hicks, L.C., Hu, B., Li, F., Liu, X., Wei, D., Wang, Z., Bao, W., 2023. Latitudinal patterns of particulate and mineral-associated organic matter down the soil profile in drylands. Soil Tillage Res. 226, 105580. https://doi.org/10.1016/j.still.2022.105580.

Limousin, G., Tessier, D., 2007. Effects of no-tillage on chemical gradients and topsoil acidification. Soil Tillage Res. 92, 167–174. https://doi.org/10.1016/j.still.2006.02.003.

Liu, B., Tu, C., Hu, S., Gumpertz, M., Ristaino, J.B., 2007. Effect of organic, sustainable, and conventional management strategies in grower fields on soil physical, chemical, and biological factors and the incidence of Southern blight. Appl. Soil Ecol. 37 (3), 202–214. https://doi.org/10.1016/j.apsoil.2007.06.007.

López-González, D., Bruno, L., Díaz-Tielas, C., Lupini, A., Aci, M.M., Talarico, E., Madeo, M.L., Muto, A., Sánchez-Moreiras, A.M., Araniti, F., 2023. Short-term effects of trans-cinnamic acid on the metabolism of zea mays L. roots. Plants 12 (1), 189.

Maeder, P., Fliessbach, A., Dubois, D., Gunst, L., Fried, P., Niggli, U., 2002. Soil fertility and biodiversity in organic farming. Science 296 (5573), 1694–1697. https://doi.org/10.1126/science.1071148.

Melero, S., Porras, J.C.R., Herencia, J.F., Madejon, E., 2006. Chemical and biochemical properties in a silty loam soil under conventional and organic management. Soil Tillage Res. 90 (1-2), 162–170.

Mikutta, R., Mikutta, C., Kalbitz, K., Scheel, T., Kaiser, K., Jahn, R., 2007. Biodegradation of forest floor organic matter bound to minerals via different binding mechanisms. Geochim. Cosmochim. Acta 71, 2569–2590. https://doi.org/10.1016/j.gca.2007.03.002.

Muruganandam, S., Israel, D.W., Robarge, W.P., 2009. Activities of nitrogen-mineralization enzymes associated with soil aggregate size fractions of three tillage systems. Soil Sci. Soc. Am. J. 73, 751–759. https://doi.org/10.2136/sssaj2008.0231.

Olchin, G.P., Ogle, S., Frey, S.D., Filley, T.R., Paustian, K., Six, J., 2008. Residue carbon stabilization in soil aggregates of no-till and tillage management of dryland cropping systems. Soil Sci. Soc. Am. J. 72, 507–513. https://doi.org/10.2136/sssaj2006.0417.

Palese, A.M., Pasquale, V., Celano, G., Figliuolo, G., Masi, S., Xiloyannis, C., 2009. Irrigation of olive groves in Southern Italy with treated municipal wastewater: effects on microbiological quality of soil and fruits. Agric. Ecosyst. Environ. 129, 43–51. https://doi.org/10.1016/j.agee.2008.07.003.

Prescott, C.E., Vesterdal, L., 2021. Decomposition and transformations along the continuum from litter to soil organic matter in forest soils. For. Ecol. Manag. 498, 119522. https://doi.org/10.1016/j.foreco.2021.119522.

Pulleman, M.M., Bouma, J., Van Essen, E.A., Meijles, E.W., 2000. Soil organic matter content as a function of different land use history. Soil Sci. Soc. Am. J. 64 (2), 689–693. https://doi.org/10.2136/sssaj2000.642689x.

R Core Team, 2020. R: a language and environment for statistical computing. R Foundation for StatisticalComputing, Vienna, Austria. ⟨https://www.r-project.org/⟩.

Rabbi, S.M.F., Minasny, B., McBratney, A.B., Young, I.M., 2020. Microbial processing of organic matter drives stability and pore geometry of soil aggregates. Geoderma 360, 114033. https://doi.org/10.1016/j.geoderma.2019.114033.

Roth, V.N., Lange, M., Simon, C., Hertkorn, N., Bucher, S., Goodall, T., Griffiths, R.I., Mellado-Vázquez, P.G., Mommer, L., Oram, N.J., Weigelt, A., Dittmar, T., Gleixner, G., 2019. Persistence of dissolved organic matter explained by molecular changes during its passage through soil. Nat. Geosci. 12 (9), 755–761.

Scarciglia, F., Critelli, S., Borrelli, L., Coniglio, S., Muto, F., Perri, F., 2016. Weathering profiles in granitoid rocks of the Sila Massif uplands, Calabria, southern Italy: new insights into their formation processes and rates. Sedimen. Geol. 336, 46–67.

Scarciglia, F., Le Pera, E., Critelli, S., 2005. Weathering and pedogenesis in the Sila Grande Massif (Calabria, South Italy): from field scale to micromorphology. Catena 61 (1), 1–29.

Sequi P. (2017) Fondamenti di chimica del suolo, Patron Editore, Bologna, 3° edizione, (2017). ISBN 978-88-555-3362-1.

Sheehy, J., Regina, K., Alakukku, L., Six, J., 2015. Impact of no-till and reduced tillage on aggregation and aggregate-associated carbon in Northern European agroecosystems. Soil Tillage Res. 150, 107–113. https://doi.org/10.1016/j.still.2015.01.015.

Sofo, A., Palese, A.M., 2021. Mediterranean olive orchard subjected to sustainable management in Matera, Basilicata, Italy. FAO, ITPS, 'Recarbonizing Global Soils – A Technical Manual of Recommended Sustainable Soil Management. Volume 4: Cropland, Grassland, Integrated Systems and Farming Approaches – Case Studies'. FAO, Rome, Italy, pp. 177–186.

Sofo, A., Ricciuti, P., Fausto, C., Mininni, A.N., Crecchio, C., Scagliola, M., Malerba, A.D., Xiloyannis, C., Dichio, B., 2019. The metabolic and genetic diversity of soil bacterial communities depends on the soil management system and C/N dynamics: the case of sustainable and conventional olive groves. Appl. Soil Ecol. 137, 21–28. https://doi.org/10.1016/j.apsoil.2018.12.022.

Tan, C.-Y., Dodd, I.C., Chen, J.E., Phang, S.-M., Chin, C.F., Yow, Y.-Y., Ratnayeke, S., 2021. Regulation of algal and cyanobacterial auxin production, physiology, and application in agriculture: an overview. J. Appl. Phycol. 33 (5), 2995–3023. https://doi.org/10.1007/s10811-021-02475-3.

Totsche, K.U., Amelung, W., Gerzabek, M.H., Guggenberger, G., Klumpp, E., Knief, C., Lehndorff, E., Mikutta, R., Peth, S., Prechtel, A., Ray, N., Kögel-Knabner, I., 2018. Microaggregates in soils. J. Plant Nutr. Soil Sci. 181, 104–136. https://doi.org/10.1002/jpln.201600451.

Van Diepeningen, A.D., De Vos, O.J., Korthals, G.W., Van Bruggen, A.H.C., 2006. Effects of organic versus conventional management on chemical and biological parameters in agricultural soils. Appl. Soil Ecol. 31 (1–2), 120–135. https://doi.org/10.1016/j.apsoil.2005.03.003.

Vieublé-Gonod, L., Benoit, P., Cohen, N., Houot, S., 2009. Spatial and temporal heterogeneity of soil microorganisms and isoproturon degrading activity in a tilled soil amended with urban waste composts. Soil Biol. Biochem. 41, 2558–2567. https://doi.org/10.1016/j.soilbio.2009.09.017.

Violante, P., 2013. Chimica e Fertilità del Suolo, 1° Ed.. Edagricole, Bologna, Italy. ISBN 978-88-506-5417-8.

Wander, M.M., Traina, S.J., 1996. Organic matter fractions from organically and conventionally managed soils: I. Carbon and nitrogen distribution. Soil Sci. Soc. Am. J. 60 (4), 1081–1087. https://doi.org/10.2136/sssaj1996.03615995006000040017x.

Whalen, E.D., Grandy, A.S., Sokol, N.W., Keiluweit, M., Ernakovich, J., Smith, R.G., Frey, S.D., 2022. Clarifying the evidence for microbial- and plant-derived soil organic matter, and the path toward a more quantitative understanding. Glob. Change Biol. 28, 7167–7185. https://doi.org/10.1111/gcb.16413.

White, A.F., 2005. Natural weathering rates of silicate minerals. In: Drever, J.I., Holland, H.D., Turekian, K.K. (Eds.), Surface And Ground Water, Weathering, And Soils Treatise. On Geochemistry. Elsevier-Pergamon, Oxford, pp. 133–168 (chapter 6).

Yeasmin, S., Singh, B., Johnston, C.T., Hua, Q., Sparks, D.L., 2023. Changes in particulate and mineral-associated organic carbon with land use in contrasting soils. Pedosphere 33, 421–435. https://doi.org/10.1016/j.pedsph.2022.06.042.

**Supplementary materials**

**Supplementary Table S1.** Soil total carbon (STC), total inorganic carbon (SIC), total nitrogen (STN), STC/STN ratio, pH (water), and bulk density in soils of the sustainable ($S_{mng}$) and conventional ($C_{mng}$) systems measured at different depths, according to Pansu and Gautheyrou (2006)*. Each value represents the mean (± SD) from composite soil composite samples ($n$ = 3). The values followed by different letters are statistically different ($p \leq 0.05$) within columns. nd = not detected.

| Soil system | Soil depth (cm) | STC (g kg$^{-1}$) | SIC (g kg$^{-1}$) | STN (g kg$^{-1}$) | STC/STN | pH | Bulk density (g cm$^{-3}$) |
|---|---|---|---|---|---|---|---|
| Sustainable ($S_{mng}$) | 0-5 | 24.19 ± 1.76 a | 2.44 ± 0.32 c | 2.38 ± 0.19 a | 10.17 ± 0.62 b | 7.61 ± 0.03 d | 1.15 ± 0.05 c |
| | 5-15 | 9.25 ± 0.60 c | 5.26 ± 0.59 b | 1.80 ± 0.91 b | 6.02 ± 2.67 d | 7.70 ± 0.06 c | 1.25 ± 0.04 bc |
| | 15-30 | 5.84 ± 0.04 d | 6.35 ± 0.45 a | 1.03 ± 0.26 b | 5.88 ± 1.33 d | 7.80 ± 0.03 bc | 1.34 ± 0.05 b |
| Conventional ($C_{mng}$) | 0-5 | 11.99 ± 0.46 b | 4.54 ± 0.38 bc | 1.10 ± 0.22 b | 11.23 ± 2.56 a | 7.85 ± 0.04 bc | 1.23 ± 0.03 bc |
| | 5-15 | 11.42 ± 0.15 bc | 4.47 ± 0.54 bc | 1.20 ± 0.07 b | 9.51 ± 0.53 c | 7.91 ± 0.05 b | 1.40 ± 0.06 a |
| | 15-30 | 9.66 ± 0.16 c | 6.86 ± 0.34 a | 1.12 ± 0.06 b | 8.65 ± 0.32 c | 8.08 ± 0.05 a | 1.48 ± 0.05 a |

* = All soil samples were air-dried at approximately 25 °C and then sieved through a 2-mm stainless steel sieve. The size fraction smaller than 2 mm was used for soil chemical analyses. Soil organic carbon (SOC) was determined by Walkley and Black method by oxidation at 170 °C with potassium dichromate ($K_2Cr_2O7$) in the presence of sulfuric acid ($H_2SO_4$), and the excess $K_2Cr_2O_7$ was measured by Möhr salt titration. Total carbonates were measured by calcimetry using hydrochloric acid and calculating the volume of released carbon dioxide at controlled temperature and pressure. Total inorganic carbon (SIC) was estimated stoichiometrically by the values of total carbonates. Soil total nitrogen (STN) was measured by the Kjeldahl method. Soil pH was measured by a glass electrode (model Basic 20®; Crison Instruments SA, Barcelona, Spain) in distilled water using a suspension 1:2.5 soil to liquid phase ratio. Bulk density was measured using volumetric rings (5 cm of internal Ø).

**Supplementary Table S2.** Output parameters of the three-way MANOVAs on STC (a), STN (b) and C/N ratio (c), considering the three fixed variables: the typology of soil management ($S_{mng}$, $C_{mng}$), the soil depth (0-5, 5-15, 15-30 cm), and the aggregate size classes (1-0.250, 0.250-0.063, <0.063 mm).

**a.**

| | **Df** | **F value** | **Pr(>F)** |
|---|---|---|---|
| **Treatment** | 1 | | |
| Conventional | 1 | 0.6541 | 0.434402 |
| Sustainable | 1 | 0.6541 | 0.434402 |
| **Depth (cm)** | 2 | | |
| 0-5 | 1 | 8.8922 | 0.004277 |
| 5-15 | 1 | 6.5161 | 0.025341 |
| 15-30 | 1 | 11.2683 | 0.005708 |
| **Aggregates (mm)** | 2 | | |
| 1-0.250 | 1 | 5.1679 | 0.024048 |
| 0.250-0.063 | 1 | 5.5764 | 0.035957 |
| <0.063 | 1 | 4.7594 | 0.049750 |
| **Treatment** | 12 | | |

**b.**

| | **Df** | **F value** | **Pr(>F)** |
|---|---|---|---|
| **Treatment** | 1 | | |
| Conventional | 1 | 5.2444 | 0.040927 |
| Sustainable | 1 | 5.2444 | 0.040927 |
| **Depth (cm)** | 2 | | |
| 0-5 | 1 | 9.5666 | 0.003279 |
| 5-15 | 1 | 8.6139 | 0.012489 |
| 15-30 | 1 | 10.5192 | 0.007043 |
| **Aggregates (mm)** | 2 | | |
| 1-0.250 | 1 | 5.4050 | 0.021200 |
| 0.250-0.063 | 1 | 5.7369 | 0.033815 |
| <0.063 | 1 | 5.0731 | 0.043810 |
| **Treatment** | 12 | | |

**c.**

| | Df | F value | Pr(>F) |
|---|---|---|---|
| **Treatment** | 1 | | |
| Conventional | 1 | 86.3392 | 7.872e-07 |
| Sustainable | 1 | 86.3392 | 7.872e-07 |
| **Depth (cm)** | 2 | | |
| 0-5 | 1 | 3.6196 | 0.05888 |
| 5-15 | 1 | 7.2216 | 0.01977 |
| 15-30 | 1 | 0.0175 | 0.89690 |
| **Aggregates (mm)** | 2 | | |
| 1-0.250 | 1 | 0.4594 | 0.64233 |
| 0.250-0.063 | 1 | 0.3288 | 0.57695 |
| <0.063 | 1 | 0.5900 | 0.45728 |
| **Residuals** | 12 | | |

**Supplementary Figure S1.** Simplified geological map of the investigated area (after Bloise et al., 2019; de Musso et al., 2020) with the location of collected sample sites.

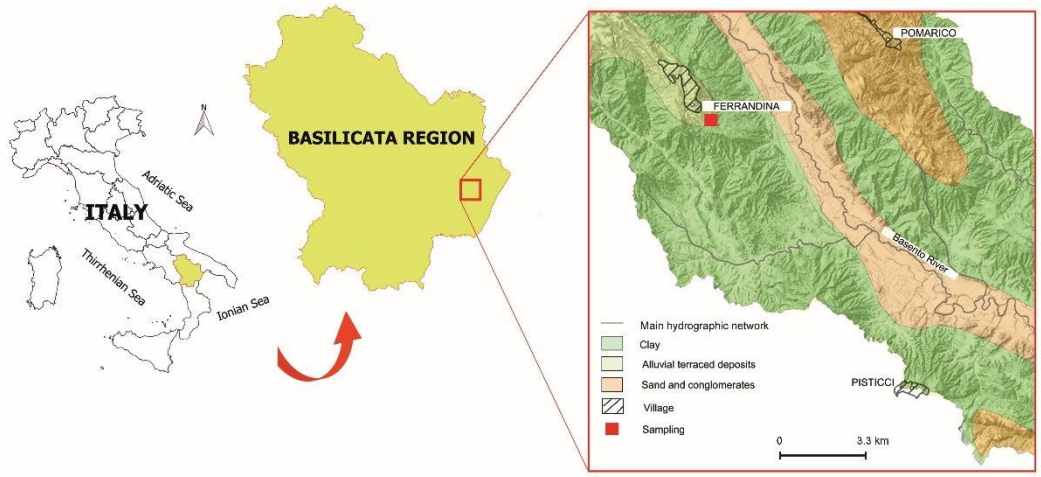

**Supplementary Figure S2. a)** The experimental orchard at soil sampling time in August 2021 and **bc)** the two systems (conventional, **b**; sustainable, **c**) in April 2021.

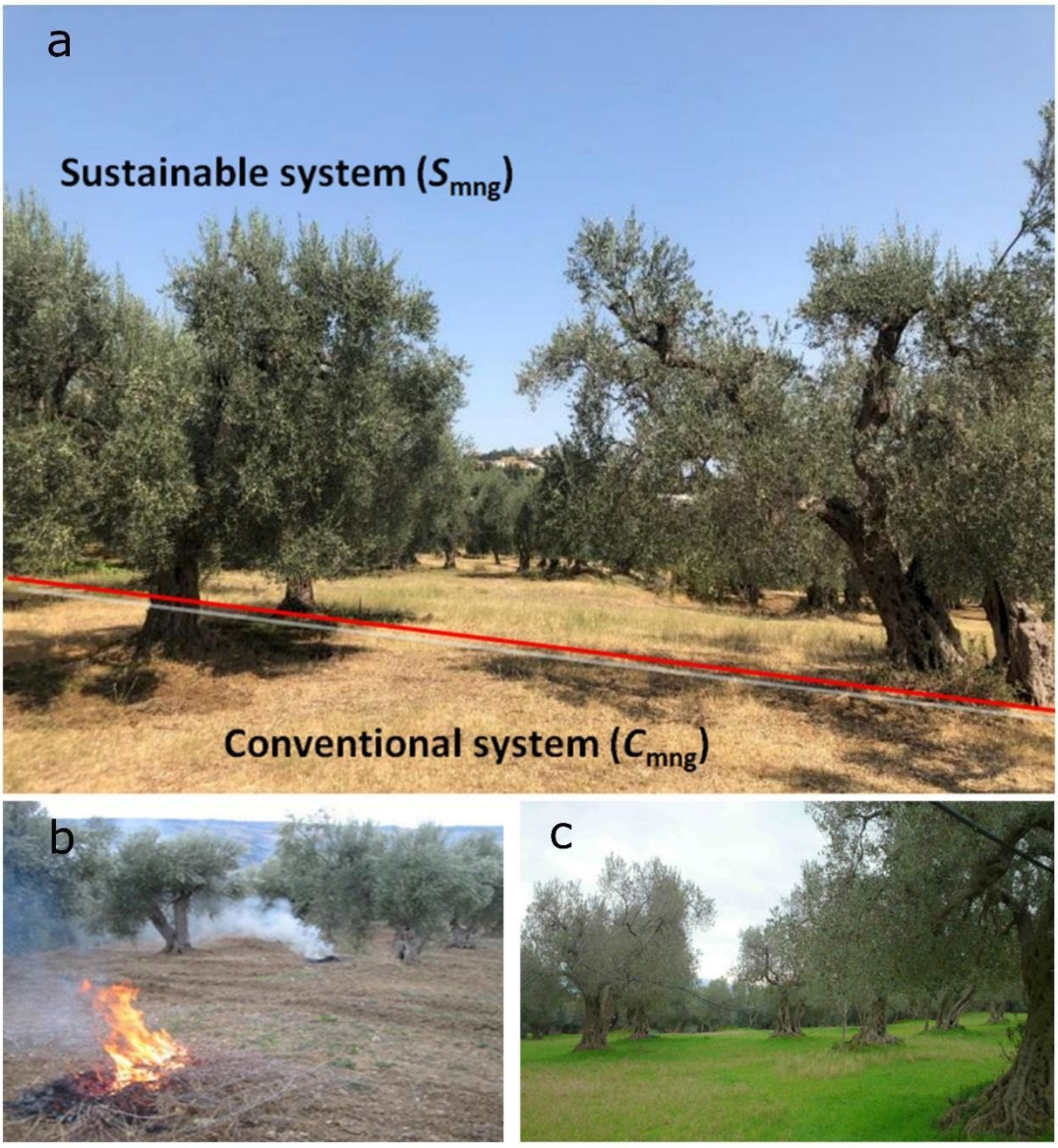

**Supplementary Figure S3.** Scheme about the different land use of the orchard based on the tillage, the mineral nutrition and the pruning and crop residuals management as reported in Table 1.

**Supplementary Figure S4. a)** Soil sampling position and method in the sustainable system ($S_{mng}$). In evidence: the drip emitters (red circle) and the distance from the trunk (yellow line). **b)** The excavated trench (yellow rectangle) and **c)** a hole at a depth of 30 cm.

**References**

Bloise, A., Ricchiuti, C., Giorno, E., Fuoco, I., Zumpano, P., Miriello, D., Apollaro, C., Crispini, A., De Rosa, R., Punturo, R., 2019. Assessment of Naturally Occurring Asbestos in the Area of Episcopia (Lucania, Southern Italy). Fibers 7, 45. https://doi.org/10.3390/fib7050045

de Musso, N.M., Capolongo, D., Caldara, M., Surian, N., Pennetta, L., 2020. Channel Changes and Controlling Factors over the Past 150 Years in the Basento River (Southern Italy). Water 12, 307. https://doi.org/10.3390/w12010307

Pansu, M., Gautheyrou, J., 2006. Handbook of Soil Analysis. Berlin, Heidelberg: Springer Berlin Heidelberg. https://doi.org/10.1007/978-3-540-31211-6